GA/EE/77-1

NAVIGATIONAL ACCURACY REQUIREMENTS OF AEROMANEUVERING SPACE VEHICLES

THESIS

GA/EE/77-1

Robert J. Chambers
Capt. USAF

AFIT/GA/EE/77-1

NAVIGATIONAL ACCURACY REQUIREMENTS OF AEROMANEUVERING SPACE VEHICLES

Master's THESIS

Presented to the Faculty of the School of Engineering

of the Air Force Institute of Technology

Air University

in Partial Fulfillment of the

Requirements for the Degree of

Master of Science

by

Robert J. Chambers B.S.

Capt USAF

Graduate Astronautical Engineering

March 1977

73 p.

Approved for public release; distribution unlimited

Preface

I became interested in the concept of the aeromaneuvering orbital transfer vehicle while doing research on Space Shuttle upper stages. The potential for increased capability over purely propulsive OTVs is so much greater as to warrant a detailed investigation.

This thesis is an extension of work performed by the Lockheed Missiles and Space Company under NASA contracts NAS8-28586 and NAS8-31452, and is based on the recommendations for future study contained in these reports. I felt qualified to examine the problems of navigational accuracy during the aeromaneuvering phase of flight since I had completed the course sequences in Navigation and in Guidance and Control at AFIT.

I would like to express my appreciation to my thesis advisor, Maj Richard M. Potter, for his advice and critical review of my work during the preparation of this report. I would also like to thank Mr J.P. Hathcoat of the Marshall Space Flight Center for his assistance during my research for this study.

Robert J. Chambers

Contents

List of Figures

Nomenclature

The MKS system is used in this study.

AMOOS - Aeromaneuvering Orbit-to-Orbit Shuttle

A_r - aerodynamic reference area = 15.69 m^2

C_d - coefficient of drag = 2.5125

C_l - coefficient of lift = 1.3457

C_1, C_2, C_3 } gain coefficients

D - drag

GEO - geosynchronous equatorial orbit

h - altitude

h_o - reference altitude = 7.315 km

L - lift

LEO - low earth orbit

m - mass of vehicle = 6804 kg

$\underline{r}$ - inertial position vector

u - unit vector or control variable

$\underline{V}$ - inertial velocity

V_r - relative velocity

V_e - inertial velocity of atmosphere

β - bank angle

β_c - commanded bank angle

β_o - nominal bank angle = 90 degrees

γ - flight path angle

θ - see Fig. 1

u - gravitational parameter

ρ - atmospheric density

ρ_c - atmospheric density at sea level

Ψ - see Fig. 1

Abstract

A preliminary investigation was conducted to determine the navigational accuracy required by the Aeromaneuvering Orbit-to-Orbit Shuttle (AMOOS) during the atmospheric phase of flight. The guidance scheme, which is the same as the one developed by Lockheed in the original AMOOS study, uses the parameters of velocity, flight path angle, and density altitude to correct to a nominal trajectory. Density altitude is obtained from atmospheric density, which is calculated from vehicle acceleration. Errors in velocity, flight path angle, and acceleration were introduced into a three-degree of freedom computer simulation of the vehicle trajectory using bank angle commands generated by the guidance equations. Deviations from standard atmospheric density were taken into account.

The maximum errors allowable that still permitted the vehicle to attain its phasing orbit apogee altitude of 720 km (±100 km) were determined. Three types of error were investigated: constant, sinusoidal, and random. For time-varying errors the frequency dependence was examined, as was cross-coupling of errors.

It was concluded that the guidance scheme can tolerate fairly large errors and still guide to an acceptable apogee altitude. The navigational accuracy required for the atmospheric phase of flight is within the capability of present day astrionics.

NAVIGATIONAL ACCURACY REQUIREMENTS OF AEROMANEUVERING SPACE VEHICLES

I. Introduction

Background

There is considerable interest in geosynchronous equatorial orbits for a variety of civil and military applications, such as communication links and surveillance. Unfortunately, it will be beyond the capability of the Space Shuttle to reach these orbits. The Orbiter vehicle is limited to an altitude of 300 km, and an upper stage is required to reach geosynchronous altitude of 35,800 km. An upper stage vehicle that has been proposed for the round trip from low earth orbit (LEO) to geosynchronous equatorial orbit (GEO) is the Space Tug. However, because of the large velocity change (ΔV) required for the round-trip mission, about 8740 m/sec, the large propellant mass fraction does not allow the vehicle to carry much payload.

An attractive alternative that has been presented by Lockheed is the Aeromaneuvering Orbit-to-Orbit Shuttle (AMOOS) (Ref 1, Ref 2). The advantage of this concept over the purely propulsive Space Tug is that part of the ΔV required for slowing and returning to LEO is provided by making a braking pass through the atmosphere. After exiting the atmosphere, a short rocket burn at apogee will raise the vehicle perigee out of the atmosphere and establish a phasing orbit for rendezvous with the Shuttle Orbiter. The total ΔV required in this case is 6413 m/sec, reducing the fuel load considerably

and allowing for two to three times the payload. The basic idea is that for a small increase in structural strength and the addition of a thermal protection system, a large savings in the amount of fuel required can be realized.

One of the problems associated with the AMOOS concept is that a very accurate atmospheric flight path is required. If the vehicle is one kilometer low, it will reenter, and if it is one kilometer too high, it will miss the apogee of its phasing orbit by thousands of kilometers.

The vehicle guidance problem is complicated by the fact that the density of the upper atmosphere varies widely at high altitudes. The density will vary from +40% to -35% from its nominal value (Ref 1:67, Ref 3:20). The AMOOS vehicle is able to compensate for off-nominal conditions by modulating its lift vector, and this aeromaneuvering ability is what differentiates this proposal from earlier ballistic trajectory concepts.

Purpose of the Study

One of the areas of the AMOOS proposal that has not been investigated so far is the accuracy required of the vehicle navigation system to successfully implement the guidance equations, and this is the subject of my thesis. I have taken the guidance scheme used in the original study and incorporated it into a trajectory simulation in which navigation system errors can be introduced.

The goal of the guidance system is to place the vehicle in an orbit with an apogee of 720 km (± 100 km). The ability of the

guidance system to accomplish this task is related to the navigational errors. The navigation parameters in the guidance calculations that are subject to errors are the vehicle velocity, flight path angle, and acceleration. In the simulation, errors in these variables are introduced in three ways: as a constant error in navigational information, as a sinusoidal error, and as a random error. The results of the simulation can be used to design a navigation system capable of supplying velocity, flight path angle, and acceleration information within the required accuracy.

Previous Investigations

A previous navigational accuracy study has been accomplished for the aerobraking return from GEO to LEO (Ref 4:33-45). However, this study examined a vehicle that followed an unguided trajectory through the atmosphere (it used aerobraking, but not aeromaneuvering). The results of this study indicated that a one-pass unguided braking maneuver was not feasible using forecast shuttle-era technology, due to the high accuracy requirements and unpredictable variations in atmospheric density.

A preliminary investigation by Lockheed of the effects of exoatmospheric navigation errors has determined that it will be necessary to position the AMOOS vehicle within a corridor of $\pm$ 3.5 km in depth prior to entry (Ref 2:73). The investigation did not include the effects of atmospheric navigation errors. These errors are the subject of this study, which solely concerns itself with navigational errors generated within the atmosphere and their effect on the guidance equations. Of course, the two studies are not independent, since the

same astrionics will most likely be used in both cases. It is expected that the astrionic equipment will include a combination of the following sensors: Inertial measurement unit (IMU), star tracker, horizon sensor, landmark tracker, and laser or conventional radar.

It is not the purpose of this study to actually design a navigation system and select the equipment used (each of which would have its own characteristic errors), but the results indicate to what tolerances the navigation system must supply information to implement the guidance scheme.

Chapter II will present the guidance law used in the study. Chapter III will be a description of the simulation, and Chapter IV covers the introduction of navigational errors. Results are presented in Chapter V, and conclusions are in Chapter VI.

II. Guidance Concept

Explanation of Method

The AMOOS vehicle is constrained to fit within the Shuttle Orbiter payload bay, and is basically a cylinder, with one end truncated into a lifting body shape. A detailed description of the vehicle is included in Appendix A. For the purpose of deriving the guidance law, it should be noted that the vehicle has a L/D ratio of from .5 to 1.0 at hypersonic velocities.

The guidance problem can be simply stated a maneuvering the vehicle so as to leave the atmosphere with just enough velocity to hit the proper apogee of the phasing orbit (720 km). This is a different problem than conventional reentry guidance, which is concerned with reducing velocity below some terminal value, with heating and dynamic pressures being the primary constraints.

The guidance method that has been proposed for AMOOS is controlling to a nominal trajectory, using a linear regulator. The lift vector is used to steer to the nominal trajectory by bank angle modulation. Bank angle, the orientation of lift, is used instead of angle of attack for lift control because the vehicle shape does not provide sufficient variation of the lift coefficient with angle of attack. This also permits the vehicle to present the same orientation into the relative wind, minimizing the surface area that must be covered by the thermal protection system.

Using bank control has an additional advantage. When the vehicle returns from geosynchronous orbit, it must also change

its inclination from zero to 28.5 degrees (the orbital inclination of the Shuttle Orbiter, and the latitude of Kennedy Space Center). A nominal bank angle of 90 degrees produces a plane change capability of approximately 7 degrees. This reduces the propulsive requirements at geosynchronous altitude for plane change ΔV. Changes in the bank angle from 90 degrees for steering corrections will reduce this plane change capability slightly.

Equations of Motion

The parameters used to generate bank angle commands are inertial velocity, flight path angle, and density, which is a function of altitude. The original derivation of the guidance law, from Reference 1, is presented here because it provides the basis for the remainder of the study. The equations of motion, in the osculating plane of the orbit, are derived as follows (Ref 1:D-1 - D-21):

$$\frac{d\underline{V}}{dt} = \underline{u}_{\parallel}\frac{dV}{dt} + \underline{u}_{\perp}V\frac{d\theta}{dt} \qquad (1)$$

where $u_{\parallel}$ = unit vector in the direction of $\underline{V}$

$u_{\perp}$ = unit vector perpendicular to $\underline{V}$

with the inertial reference frame as shown in Fig.1.

Summing the forces in the direction of V gives

$$-D - \frac{\mu}{r^2}m \sin\gamma = m\dot{V} \qquad (2)$$

or $$\dot{V} = -\frac{D}{m} - \frac{\mu}{r^2}\sin\gamma \qquad (3)$$

Summing the components perpendicular to $\underline{V}$ gives

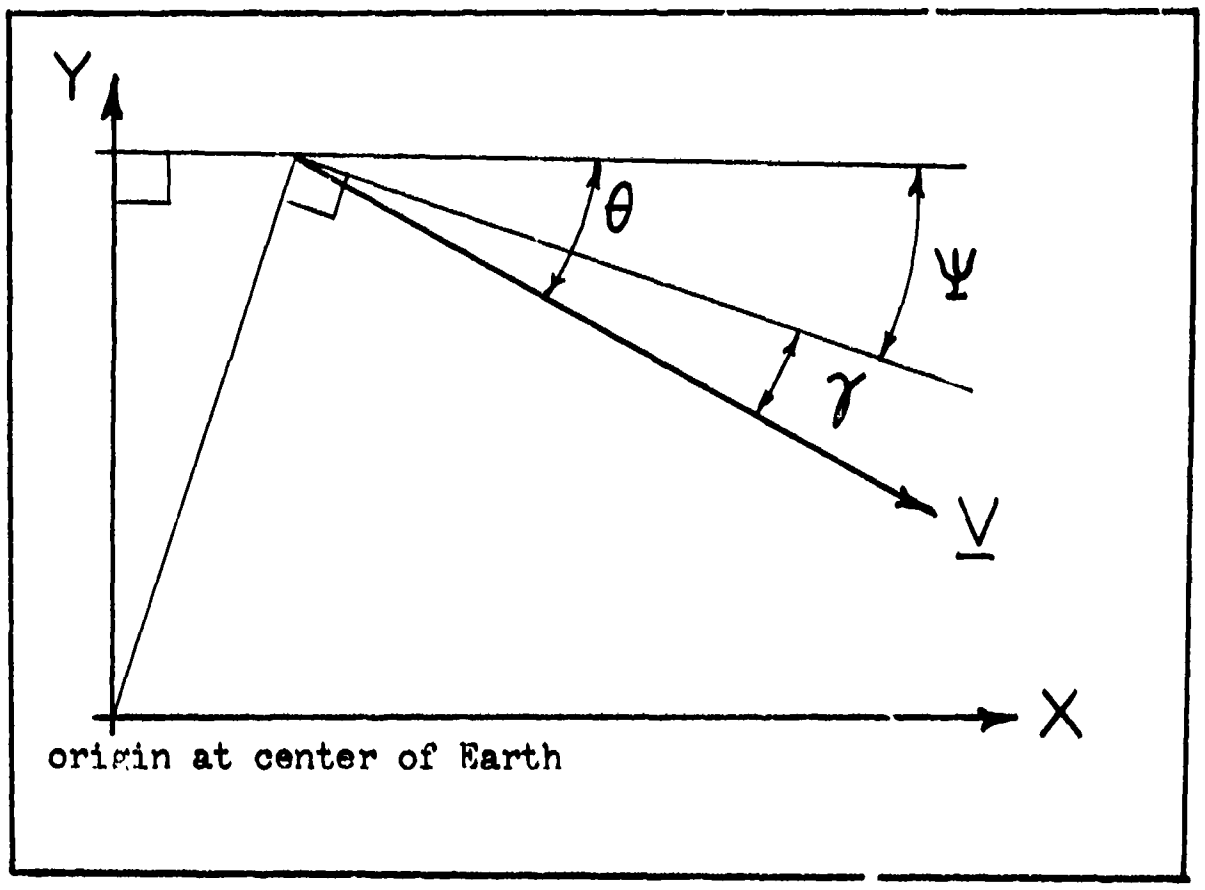

Fig. 1 - Inertial Coordinate Frame

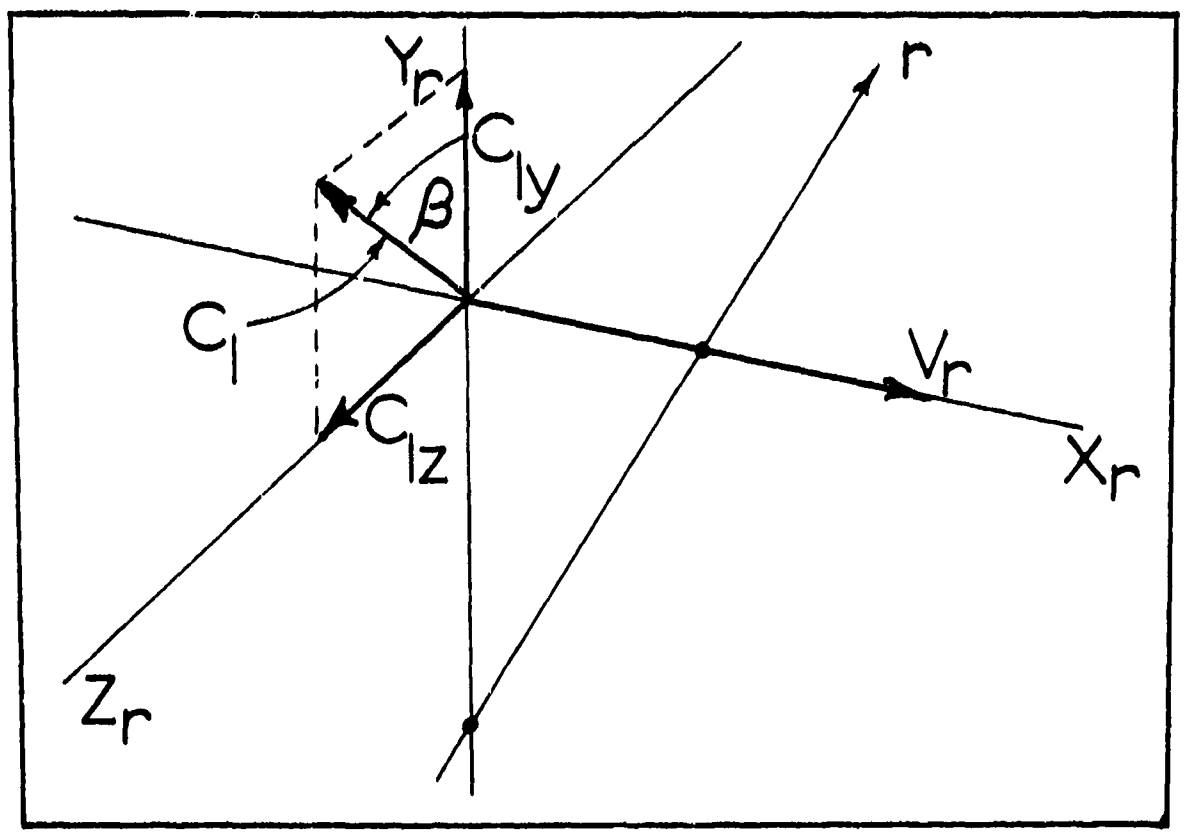

Fig. 2 - Definition of Bank Angle, β, (Y_r lies in the vertical plane formed by the radius vector r and V_r)

$$L - \frac{\mu}{r^2} m \cos \gamma = m V \dot{\theta} \tag{4}$$

As can be seen from Fig. 1

$$\dot{\theta} = \dot{\psi} + \dot{\gamma} \tag{5}$$

$$\dot{\psi} = - \frac{V \cos \gamma}{r} \tag{6}$$

Combining (5) and (6) gives

$$\dot{\theta} = \dot{\gamma} - \frac{V}{r} \cos \gamma \tag{7}$$

Substituting (7) into (4) and solving for γ yields

$$\dot{\gamma} = \frac{L}{mV} - \frac{1}{V} \left[\frac{\mu}{r^2} - \frac{V^2}{r} \right] \cos \gamma \tag{8}$$

The derivative of radial distance r is given by

$$\dot{r} = V \sin \gamma = \dot{h} \tag{9}$$

If the states of the system are taken to be V,γ, and h, then equations (3), (8), and (9) provide the state equations.

Although the lift and drag force directions are referenced to inertial velocity, they may be approximated by the force directions with respect to the vehicle velocity relative to the atmosphere since the directions of relative velocity and inertial velocity are almost parallel during the period of atmospheric flight.

Thus

$$D \simeq \tfrac{1}{2} \rho V_r^2 A_r C_d \tag{10}$$

$$L \approx \tfrac{1}{2} \rho V_r^2 A_r C_l \cos \beta \tag{11}$$

$$V_r \approx V - V_e \tag{12}$$

where bank angle, β, is defined in Fig. 2.

Control of the vehicle is accomplished by rotating the lift vector through a bank angle β, which changes the component of lift C_l in the Y_r direction, as shown in Fig. 2. The relation between β and the vehicle orientation is shown in Fig. 14, Appendix A. The control variable, u, is defined as the deviation of the commanded value of C_{ly} from some nominal value of bank, i.e.,

$$u = C_{ly} - C_{ly_o} = C_l (\cos \beta_c - \cos \beta_o) \tag{13}$$

where β_o = 90 degrees for maximum plane change capability.

Substituting (10), (11), (12), and (13) into equations (3) and (8) and assuming $\beta = \beta_c$ results in the revised equations of motion:

$$\dot{V} = - \frac{1}{2m} \rho (V - V_e)^2 C_d A_r - \frac{\mu}{r^2} \sin \gamma \tag{14}$$

$$\dot{\gamma} = \frac{1}{2mV} \rho (V - V_e)^2 A_r \left[C_l \cos \beta_o + u \right] - \left[\frac{\mu}{r^2} - \frac{V}{r} \right] \cos \gamma \tag{15}$$

$$\dot{r} = V \sin \gamma \tag{16}$$

where density is an exponential approximation according to

$$\rho = \rho_o e^{-(h/h_o)} \tag{17}$$

These equations (with u=0) are integrated from initial conditions selected to result in an apogee altitude of 720 km. Since entry altitude is fixed (at 120 km), all possible initial

conditions consistent with the transfer orbit from GEO may be specified in terms of a vacuum perigee, which can be adjusted to give the desired apogee. This integration will provide a V_{nom}, γ_{nom}, and h_{nom} that the vehicle can be controlled to, according to the linear state feedback control law

$$u = C_1 (V - V_{nom}) + C_2 (\gamma - \gamma_{nom}) + C_3 (h - h_{nom}) \qquad (18)$$

The time-varying coefficients C_1, C_2, and C_3 are the solution to the linear regulator problem presented in the next section. The values of C_1, C_2, C_3, V_{nom}, γ_{nom}, and h_{nom} can be precomputed for discrete time intervals and stored in the on-board computer.

Linear Regulator Problem

The developement of the linear regulator problem involves a linearization of the equations of motion to the form of

$$\begin{bmatrix} \delta\dot{V} \\ \delta\dot{\gamma} \\ \delta\dot{r} \end{bmatrix} = [A] \begin{bmatrix} \delta V \\ \delta\gamma \\ \delta r \end{bmatrix} + [B] \; u \qquad (19)$$

where

$$[A] = \begin{bmatrix} \frac{\partial\dot{V}}{\partial V} & \frac{\partial\dot{V}}{\partial\gamma} & \frac{\partial\dot{V}}{\partial r} \\ \frac{\partial\dot{\gamma}}{\partial V} & \frac{\partial\dot{\gamma}}{\partial\gamma} & \frac{\partial\dot{\gamma}}{\partial r} \\ \frac{\partial\dot{r}}{\partial V} & \frac{\partial\dot{r}}{\partial\gamma} & \frac{\partial\dot{r}}{\partial r} \end{bmatrix} \qquad (20)$$

and

$$[B] = \begin{bmatrix} \frac{\partial \dot{V}}{\partial u} \\ \frac{\partial \dot{\gamma}}{\partial u} \\ \frac{\partial \dot{r}}{\partial u} \end{bmatrix} \tag{21}$$

The matrices A and B are evaluated along the nominal trajectory. The partial derivatives are calculated from equations (14), (15), and (16) as follows:

$$\frac{\partial \dot{V}}{\partial V} = -\frac{\rho}{m} V_r C_d A_r \tag{22}$$

$$\frac{\partial \dot{V}}{\partial \gamma} = -\frac{\mu}{r^2} \cos \gamma \tag{23}$$

$$\frac{\partial \dot{V}}{\partial r} = -\frac{1}{2m} V_r^2 C_d A_r \frac{\partial \rho}{\partial r} + \frac{2\mu}{r^3} \sin \gamma \tag{24}$$

$$\frac{\partial \dot{\gamma}}{\partial V} = \frac{1}{mV} \left[V_r - \frac{V_r^2}{2V} \right] \rho A_r \left[C_l \cos \beta_o + u \right] + \left[\frac{\mu}{V^2 r^2} + \frac{1}{r} \right] \cos \gamma \tag{25}$$

$$\frac{\partial \dot{\gamma}}{\partial \gamma} = \left[\frac{\mu}{V_r^2} - \frac{V}{r} \right] \sin \gamma \tag{26}$$

$$\frac{\partial \dot{\gamma}}{\partial r} = \frac{1}{2mV} V_r^2 A_r \left[C_l \cos \beta_o + u \right] \frac{\partial \rho}{\partial r} - \left[-\frac{2\mu}{V r^3} + \frac{V}{r^2} \right] \cos \gamma \tag{27}$$

$$\frac{\partial \dot{r}}{\partial V} = \sin \gamma \tag{28}$$

$$\frac{\partial \dot{r}}{\partial \gamma} = V \cos \gamma \tag{29}$$

$$\frac{\partial \dot{r}}{\partial r} = 0 \tag{30}$$

$$\frac{\partial \dot{V}}{\partial u} = 0 \tag{31}$$

$$\frac{\partial \dot{\gamma}}{\partial u} = \frac{1}{2mV} \rho V_r^2 A_r \tag{32}$$

$$\frac{\partial \dot{r}}{\partial u} = 0 \tag{33}$$

and

$$\frac{\partial \dot{\rho}}{\partial r} = -\frac{\rho_o}{h_o} \tag{34}$$

Using standard optimal control techniques (Ref 5:209), a performance index is chosen to minimize the error in phasing orbit apogee. This index of performance (which is to be minimized) consists of the terminal miss which relates directly to the square of the apogee error, plus the integral of the square of the control variable u, over the nominal flight time. This last term tends to limit the control, hence limiting the amount of propellant required for the reaction control system.

Therefore,

$$J = \frac{1}{2} \delta \underline{x}^T(t_f) \, H \, \delta \underline{x}(t_f) + \frac{1}{2} \int_{t_o}^{t_f} (u^2 R) \, dt \tag{35}$$

where

$$\delta \underline{x} = \begin{bmatrix} \delta V \\ \delta \gamma \\ \delta r \end{bmatrix} \tag{36}$$

and H and R are weighting matrices, and t_o=t_{entry} and t_f=$t_{nom\ exit}$.

The solution to the optimization problem is given by

$$u = - R^{-1} B^T K \delta\underline{x} = \underline{C}^T \delta\underline{x} \tag{37}$$

where K is given by the Riccati differential equation

$$\dot{K} = -A^T K - K A + K B R^{-1} B^T K \tag{38}$$

which is integrated backwards through time from its final conditions, $K(t_f) = H$.

Weighting Matrices

The matrix H is chosen to minimize the effect of the final state, $\delta\underline{x}(t_f)$, at atmospheric exit, on apogee altitude h_a. For small variations, δh_a can be related to the final state by

$$\delta h_a = \left[\frac{\partial h_a}{\partial V} \delta V + \frac{\partial h_a}{\partial \gamma} \delta\gamma + \frac{\partial h_a}{\partial r} \delta r \right]_{t=t_f} \tag{39}$$

The matrix H is determined by

$$\delta h_a^2 = \delta\underline{x}^T(t_f) \, H \, \delta\underline{x}(t_f) \tag{40}$$

which yields the elements h_{ij} of H:

$$h_{11} = \left(\frac{\partial h_a}{\partial V} \right)^2 \tag{41}$$

$$h_{22} = \left(\frac{\partial h_a}{\partial \gamma} \right)^2 \tag{42}$$

$$h_{33} = \left(\frac{\partial h_a}{\partial r} \right)^2 \tag{43}$$

$$h_{12} = h_{21} = \frac{\partial h_a}{\partial V} \quad \frac{\partial h_a}{\partial \gamma} \tag{44}$$

$$h_{13} = h_{31} = \frac{\partial h_a}{\partial V} \frac{\partial h_a}{\partial r} \tag{45}$$

and

$$h_{23} = h_{32} = \frac{\partial h_a}{\partial \gamma} \frac{\partial h_a}{\partial r} \tag{46}$$

Evaluating the partial derivatives at the nominal conditions at the final time (V=7980 m/sec, γ =1.75 deg, and r=6,498,153 m) results in numerical values of

$$\frac{\partial h_a}{\partial V} = 3.32 \frac{km}{m/sec}$$

$$\frac{\partial h_a}{\partial \gamma} = 74.73 \frac{km}{deg}$$

$$\frac{\partial h_a}{\partial r} = 3.116 \frac{m}{m}$$

The function R(t) was selected to prevent the peaking of the gains at perigee, the period of maximum control effectiveness. The function selected is shown in Fig. 3.

The feedback gain vector derived from eq. (37) is shown in Fig. 4. In Figures 3 and 4, the point at which time t=0 is when the vehicle passes through 95.4 km upon entry. Above this altitude there is not sufficient atmosphere to permit control effectiveness.

In the region of atmospheric guidance, the vehicle acceleration is primarily affected by the drag terms. Therefore, neglecting the gravitational terms, and for small flight path angles, from eq. (14)

$$m \dot{V} = \tfrac{1}{2} \rho V_r^2 C_d A_r \tag{47}$$

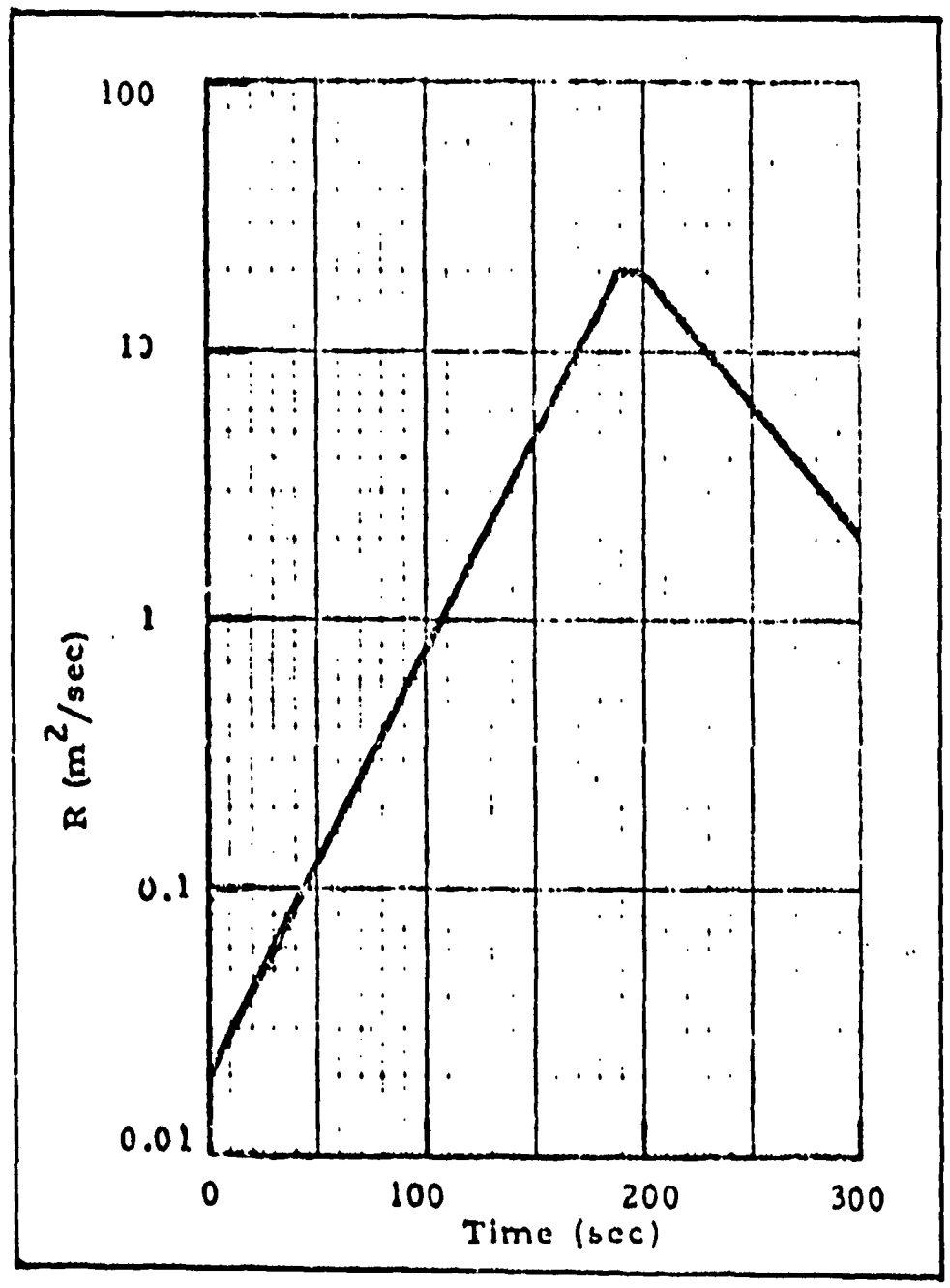

Fig. 3 - Weighting Coefficient R (Ref 2: D-11)

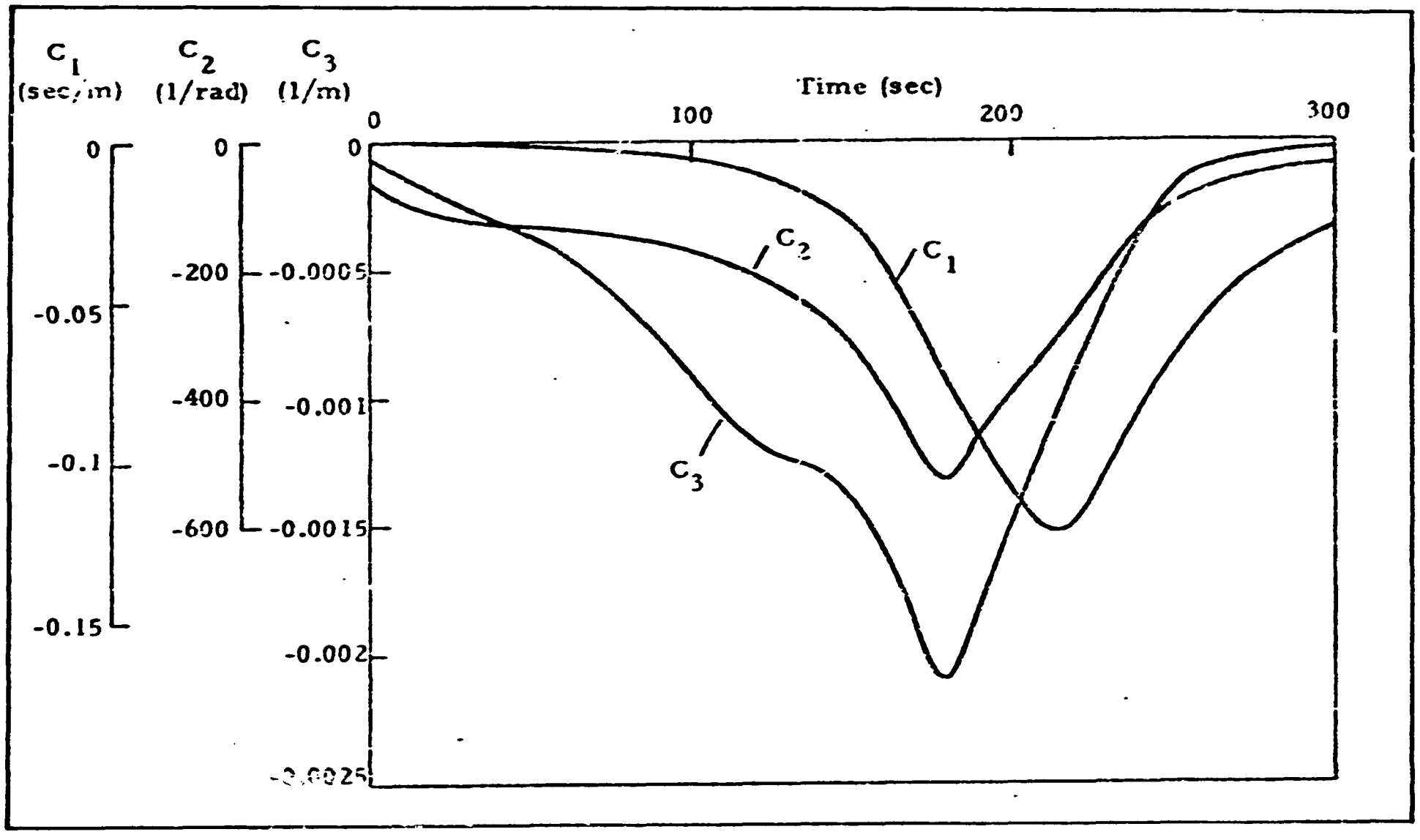

Fig. 4 - Feedback Gain Vector $\underline{C}$ for AMOOS Guidance (Ref 2: D-12)

or

$$\rho = \frac{-2\ \dot{V}\ m}{V_r^2\ C_d\ A_r} \tag{48}$$

This density can be related to an altitude through the use of eq.(17)

$$h = -\ h_o\ \ln(\ \rho/\rho_o\ ) \tag{49}$$

Thus, from measuring vehicle acceleration, a density altitude can be calculated. This is compared to the nominal density altitude to determine the vehicle altitude error.

III. Description of Simulation

Purpose

The validity of the guidance scheme is tested by a computer program which simulates the actual vehicle dynamics with guidance commands. Perturbations from the nominal trajectory are introduced to determine how well the guidance law will correct back to the nominal. In the case under study, perturbations are caused by deviations in atmospheric density and by errors in the calculated position and velocity information supplied by the vehicle's navigation system. Atmospheric density fluctuations are known to vary from -35% to 40% from normal in the region flown by AMOOS (from 120 to 70 km), and are easily input to the simulation. Navigational errors can also be easily input to the simulation and these error sources are described in the next chapter.

Assumptions

The following assumptions have been made in constructing the vehicle simulation:

1. The assumptions of a spherical rotating earth and atmosphere.
2. The atmospheric density can be modeled as an exponential function of altitude.
3. The vehicle is returning from GEO via a Hohmann transfer orbit with a 21.5 degree plane change, with a targeted vacuum perigee of 71.1 km. This value for perigee is the result of adjusting vacuum perigee to determine the initial entry conditions that result in an apogee of 720 km.

4. Vehicle flies constant angle of attack with lift, longitudinal vehicle axis, and relative wind always in the same plane. The orientation of this plane (β) is the only vehicle control that affects translational dynamics.

5. The actual bank angle is equal to the commanded bank angle.

It was originally intended to simulate an autopilot in the guidance loop to implement the bank commands, and to account for the vehicle's inability to instantly assume the commanded value. However, from the results of the simulation, the guidance commands are fairly continuous, and the value of ($\beta - \beta_c$) is small (about 2 - 3 degrees). This permits the vehicle to assume the value of β_c within the guidance cycle time (4 sec), assuming an angular acceleration of 1 deg/sec^2.

Equations of Motion

Since it was desired to examine the three-dimensional vehicle motion rather than just the motion in the osculating orbital plane, the equations of motion used in generating the guidance law could not be used. A different (although consistant) set of equations was used, based on a inertial geocentric-equatorial (IJK) coordinate system. The IJK reference frame was oriented with the I direction in the direction of the vacuum perigee, to simplify the transformation from perifocal coordinates to IJK coordinates. These equations are the same as used in the original study (Ref 1:A-3).

The vector equation of motion is:

$$\ddot{\underline{r}} = -\frac{\mu}{|\underline{r}|^3}\underline{r} + \tfrac{1}{2}\rho V_r^2 \frac{A_r C_l}{m}\hat{L} + \tfrac{1}{2}\rho V_r^2 \frac{A_r C_d}{m}\hat{D} \qquad (50)$$

where $\hat{L}$ and $\hat{D}$ are the unit vectors in the directions of lift and drag, respectively

$$\hat{L} = \frac{\underline{V}_r \times (\underline{r} \times \underline{V}_r)}{|\underline{V}_r|^2 \, |\underline{r}|} \cos \beta + \frac{(\underline{r} \times \underline{V}_r)}{|\underline{V}_r| \, |\underline{r}|} \sin \beta \qquad (51)$$

and

$$\hat{D} = - \frac{\underline{V}_r}{|\underline{V}_r|} \qquad (52)$$

The aerodynamic coefficients C_l and C_d and the vehicle specifications of mass, m, and reference area, A_r, are taken from the design of Reference 2. Relative velocity, V_r, is defined by eq. (12). Bank angle, β, comes from the guidance law (eq. (18)), and the density altitude, h, is computed from eqs. (48) and (49). The program uses a Runge-Kutta integration algorithm to integrate the equations of motion from atmospheric entry to exit (120 km).

Computer Program

A flow chart of the major elements of the computer program is shown in Fig. 5. A listing of the program is included in Appendix B. The program first generates the nominal trajectory, using the equations of Chapter II. The vector of time-varying guidance coefficients is input as data points, and an interpolating table look-up routine is used to reconstruct the curves of Fig. 4 and select values for a given flight time. The elements V, γ, and r of the the osculating orbit at r = 120 km are converted to inertial position and velocity and are used as initial conditions for the integration of the equations of motion given in the previous section.

Simulated navigation errors in V, γ, and acceleration are input to the guidance section, which then generates a bank angle. The integration proceeds until the vehicle leaves the atmosphere

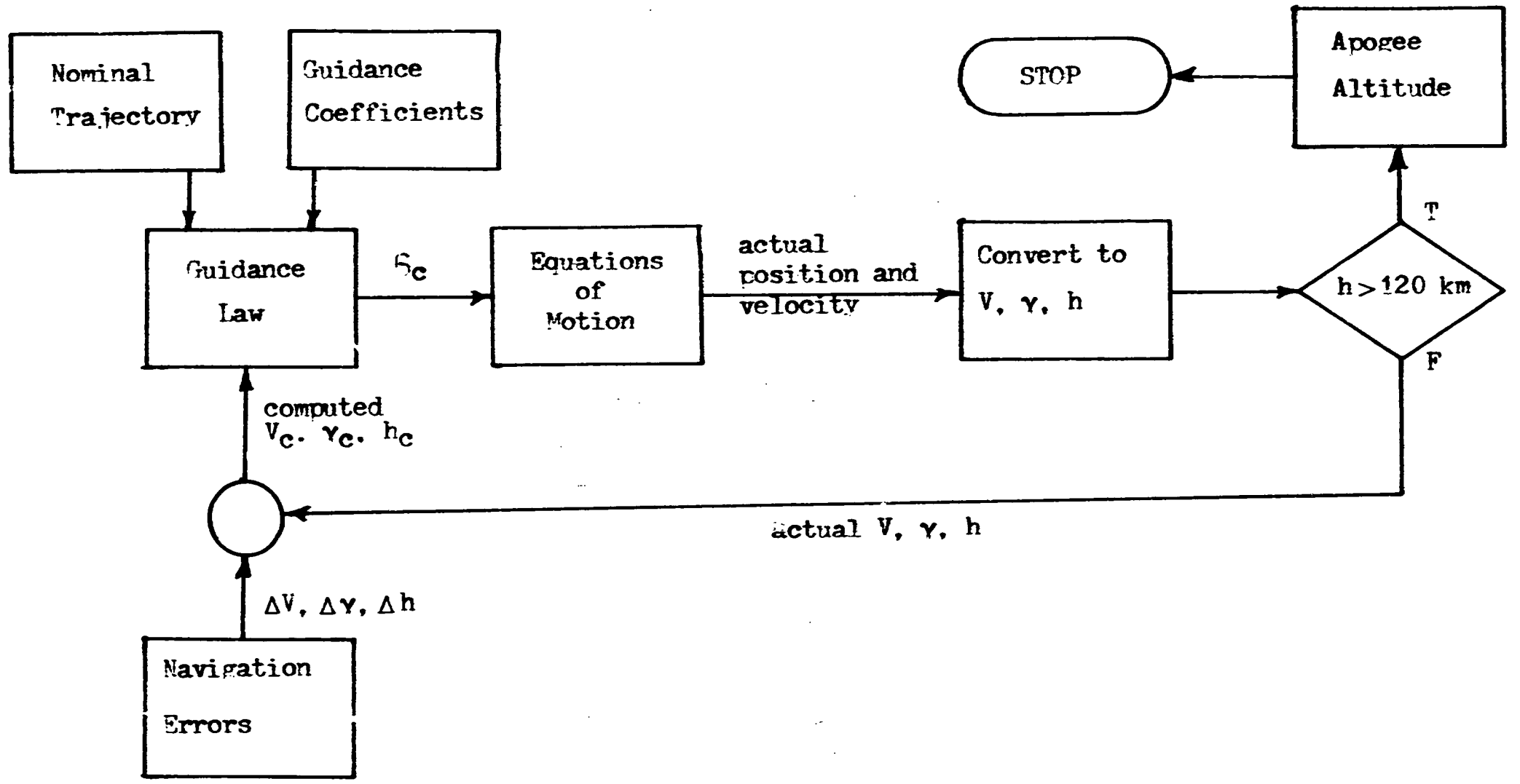

Fig. 5. Flow Chart of Simulation

(when it again reaches 120 km). At this point the apogee of the phasing orbit is calculated, assuming two body dynamics.

The integration time step is 1 second, which was determined to give good accuracy without resulting in excessive computational time. New guidance commands are generated every 4 seconds, and bank angle commands are limited to ± 30 degrees about the nominal 90 degree bank angle. The guidance cycle time and maximum bank angle represent the values that gave the best results in the original simulation work done by Lockheed. A sample trajectory is given in Appendix C.

IV. Navigation System Errors

It was attempted to model errors in a manner that would be typical of the outputs from the navigation system. Accordingly, the errors were input to the simulation as a constant (bias) error, a sinusoidal error, and as a random error. Each type of error was run with varying magnitudes to determine its relation with the output, apogee error. In addition, each error in velocity, flight path angle, and acceleration was considered for three different atmospheric density profiles. The first profile was the nominal density, and the second and third profiles were the worst-case situations of density being 40% greater than normal, and being 35% less than normal. This demonstrates the capability of the guidance system to correct for off-nominal atmospheric conditions, in addition to navigation errors.

The sinusoidal errors were run at varying frequencies to determine if there was any frequency-sensitivity in the guidance system. The range of frequencies to be examined was determined by the guidance cycle time and total time of flight. The high frequency limit was chosen to give a period equal to the guidance cycle time of 4 seconds. Any frequency greater than this would appear as a random error to the simulation. The low frequency limit was selected to give a period approximately equal to the time of atmospheric flight (400 seconds). A frequency much lower than this would appear to be almost a constant error.

The effects of random errors in velocity on apogee altitude were examined to determine if there was any significant difference between

the results for random errors and sinusoidal or constant errors. The random errors were produced using the random-number utility subprogram of the computer system. A uniformly distributed random sequence of numbers between -1 and +1 was assigned to the elements of an array at a discrete interval. This interval, which could be varied, was called the correlation time. The elements of the array between these intervals were filled in using a linear function between the random end points of the interval. The elements of the array were multiplied by the appropriate error magnitude and then each element corresponded to an error value at each cycle of the guidance equations. The use of the correlation time provided a means of varying the rate at which the random errors were input to the simulation.

The correlation time was analogous to the period of the sinusoidal errors, and so the range of correlation times was chosen from 4 to 400 seconds, using the same reasoning as was used to determine the frequency of sinusoidal errors.

Errors in each parameter were first examined independently, but the effects of cross-coupling of errors were also examined. This was to determine if the principle of superposition would be applicable to the error sources.

The results of the study are presented in the next chapter.

V. Results

Constant Error

The nominal trajectory produced by eqs. (14), (15), and (16) resulted in an apogee altitude of exactly 720 km. However, when this trajectory was "flown" in the three-dimensional simulation using eqs. (50), (51), and (52), with no errors input, it consistently yielded an apogee altitude of 730 km. This 10 km bias probably results from the different methods of calculating V_e in each case. In the case of the nominal trajectory, it is approximated, since the orientation of the osculating orbit is not known, while in the 3-D simulation it is calculated exactly. This bias was taken into account when determining the results of the navigational errors.

Errors in apogee due to errors in measured inertial velocity exhibit a linear relationship, as shown in Fig. 6. The horizontal lines show the permissible variation ($\pm$ 100 km) in apogee altitude, and the three diagonal lines show the three cases of atmospheric density being equal to nominal, and +40% and -35% from nominal.

From the figure, taking into account the 10 km bias and the possible variation in atmospheric density, it can be determined that the allowable error in measuring velocity is $\pm$ 22 m/sec. A sensitivity coefficient of -4.25 km/m/sec can be calculated for constant errors (meaning that a +1 m/sec error in measuring velocity will result in an apogee error of -4.25 km).

Figure 7 shows the effects of a constant error in measured flight path angle. This time, however, the effects are seen to be

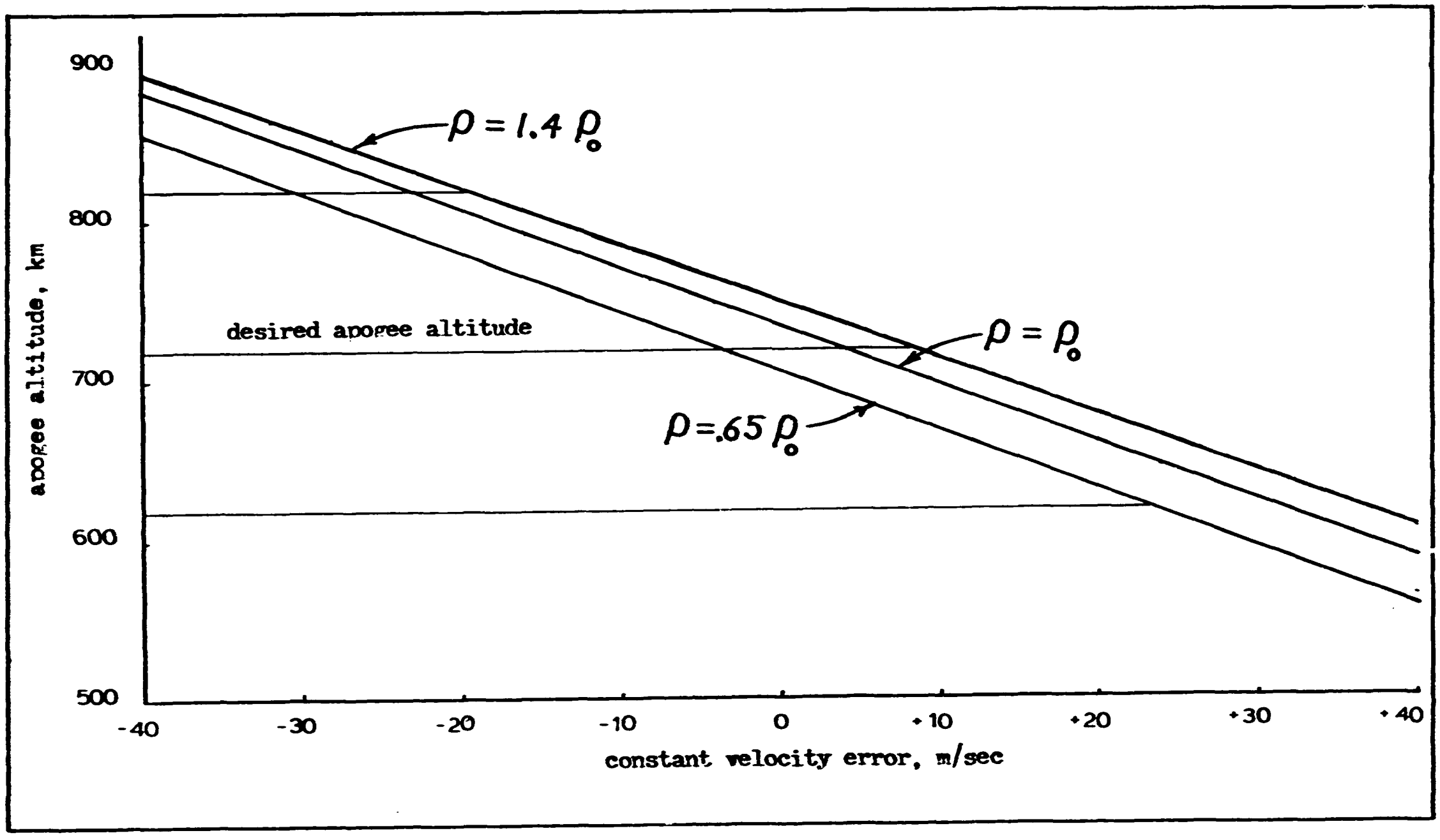

Fig. 6. Constant Velocity Errors

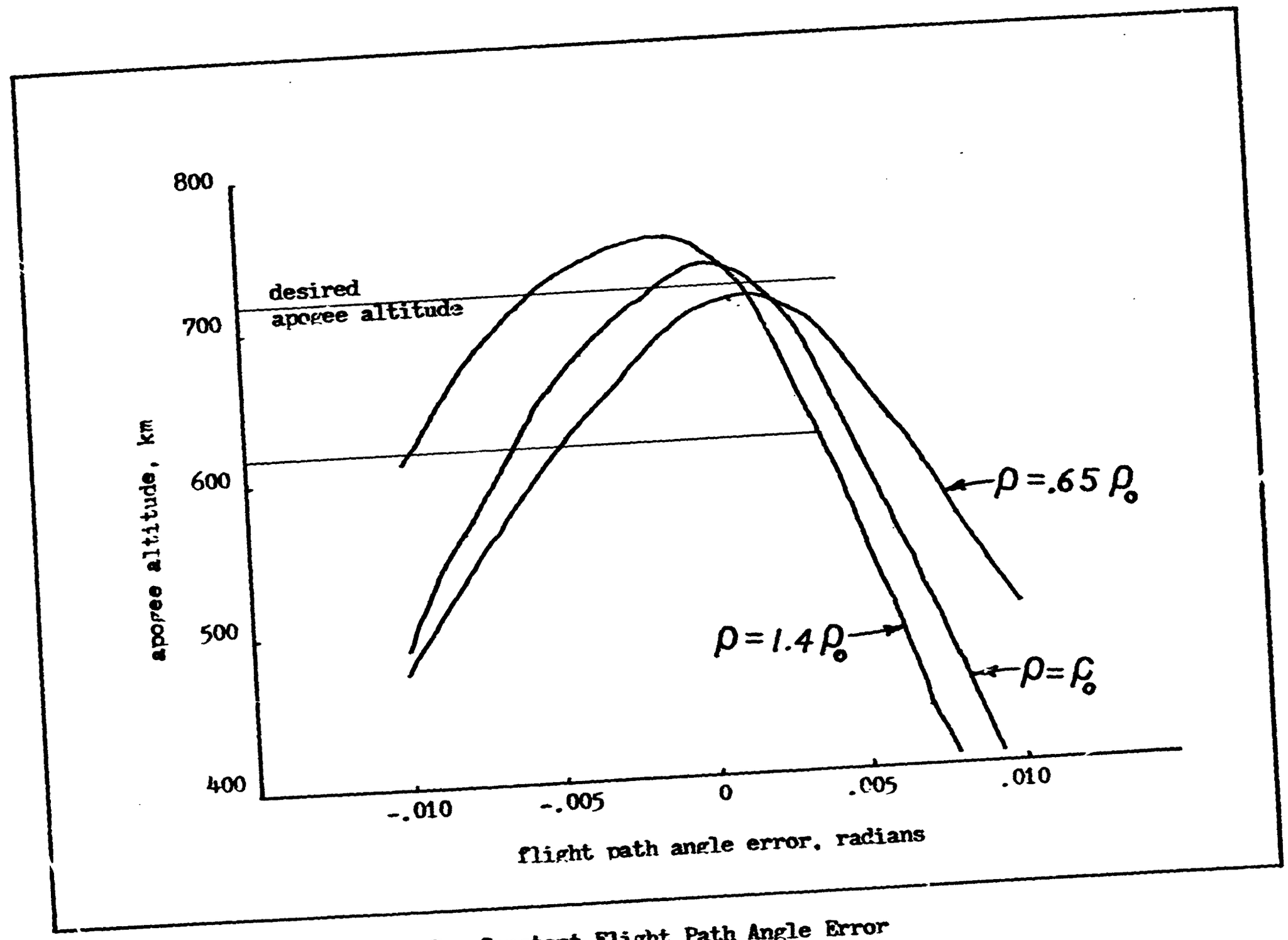

Fig. 7. Constant Flight Path Angle Error

non-linear. The maximum allowable errors, again allowing for the bias error, can be seen to be -.0045 and .0035 (-.26 deg and .20 deg). A linear sensitivity coefficient cannot be determined for these curves.

Errors in measuring acceleration result in the apogee error shown in Fig. 8. The curves indicate that acceleration errors must be kept between ± .6 m/sec^2. The curves can reasonably be approximated by a straight line in a small region, permitting the calculation of an approximate sensitivity coefficient. For the region of ±.5 m/sec^2 error, the sensitivity coefficient is 120 km/m/sec^2.

Sinusoidal Error

Sinusoidally-varying errors in velocity, flight path angle, and acceleration were input to the simulation at several different amplitudes for each of the three atmospheric density profiles. Typical results are presented in Figures 9, 10, and 11. These are for the nominal density profile, with amplitude of the errors being respectively 20 m/sec, .004 radians, and .4 m/sec^2.

The figures will be discussed together, since they all indicate the same trend. The data is plotted as discrete points because it did not lend itself to fitting a smooth curve between the points. It can be seen that at frequencies greater than .1 rad/sec the apogee deviations are small compared to the deviations produced with constant errors of the same magnitude. Below .1 rad/sec the deviations increase erratically until they are approximately the same as for constant error. This is most likely due to the guidance scheme being more sensitive to errors at one point in the flight path (probably perigee, since this is the region of greatest

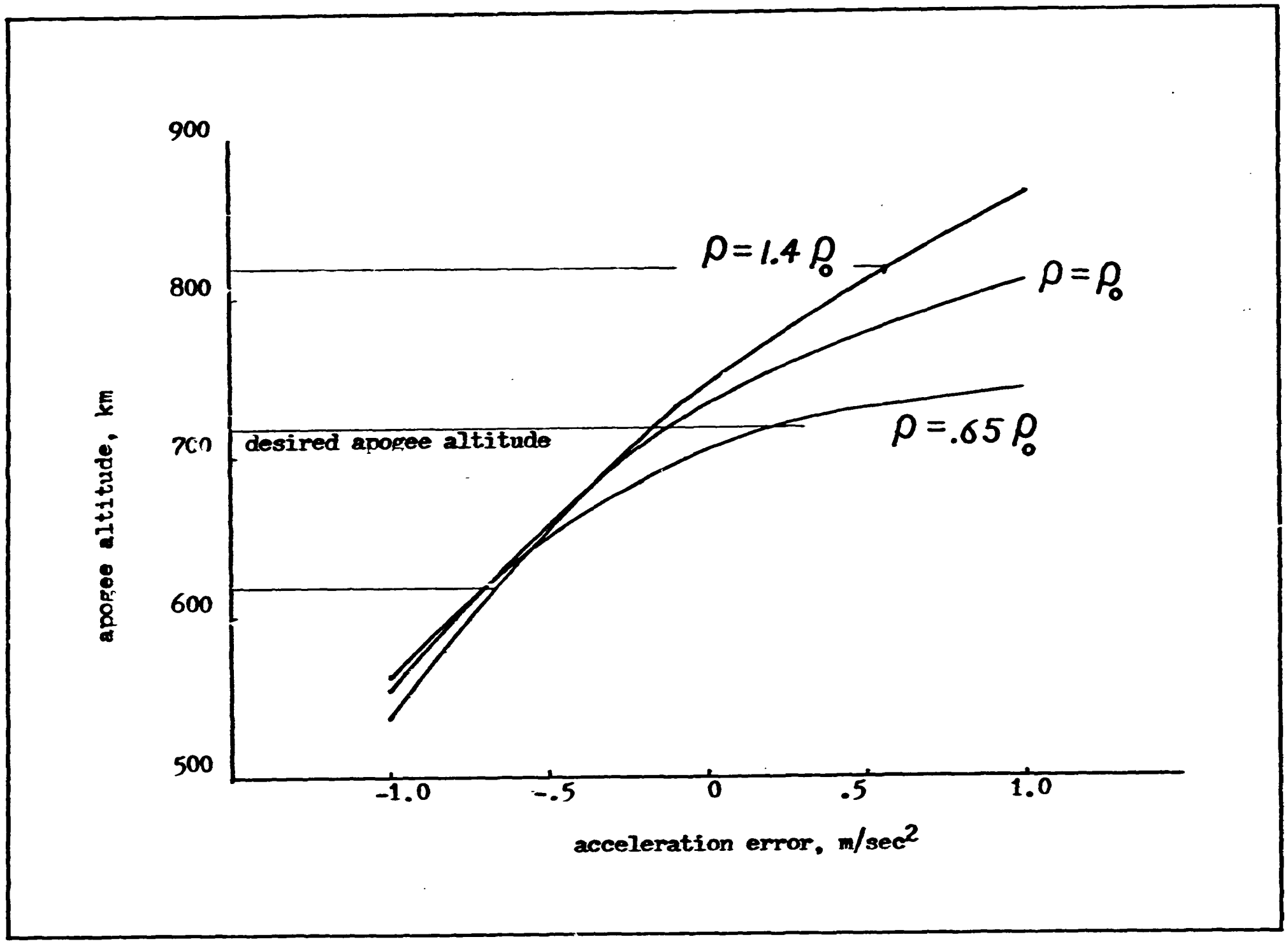

Fig. 8. Constant Acceleration Error

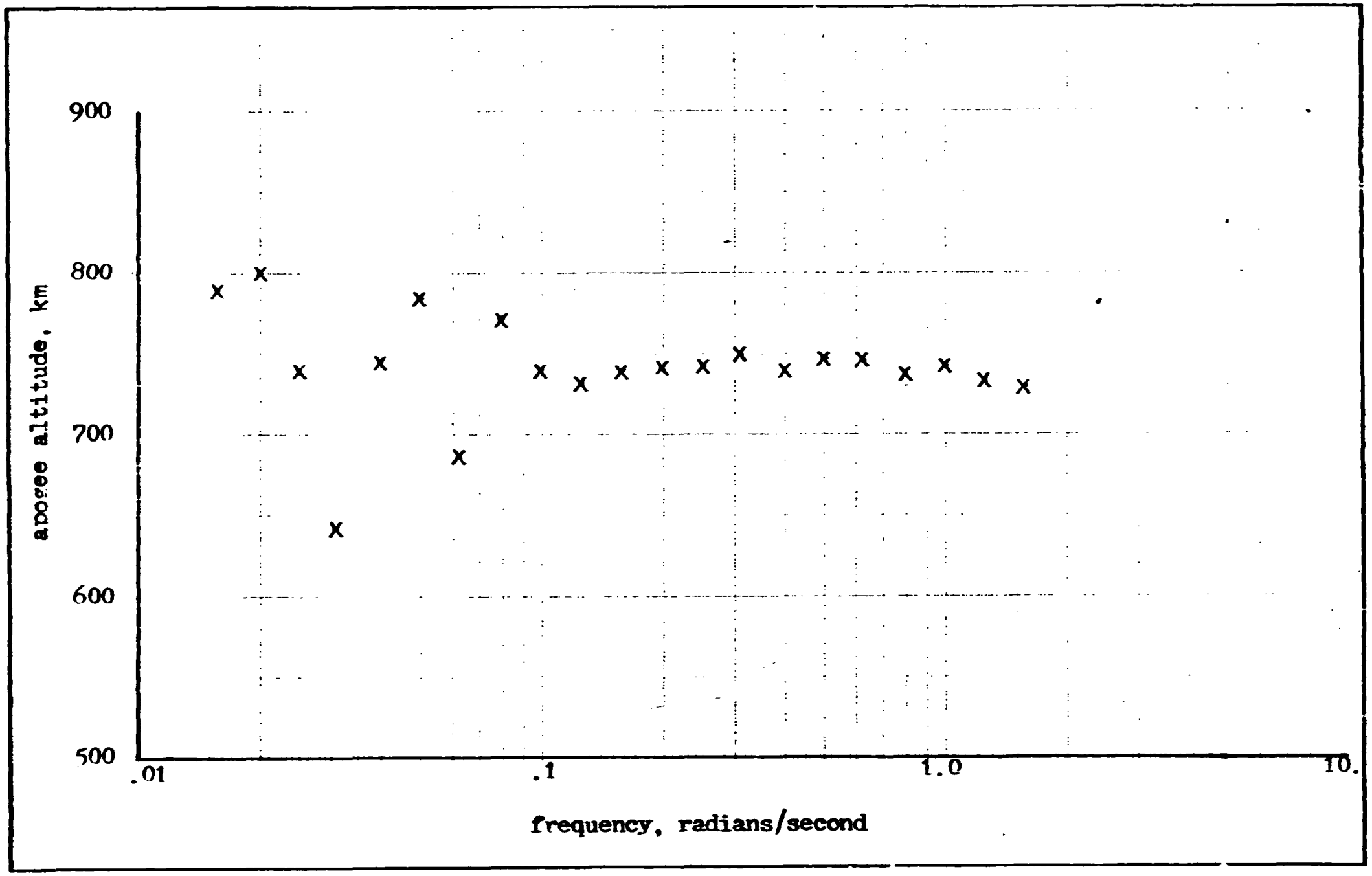

Fig. 9. Sinusoidal Velocity Errors (amplitude = 20 m/sec)

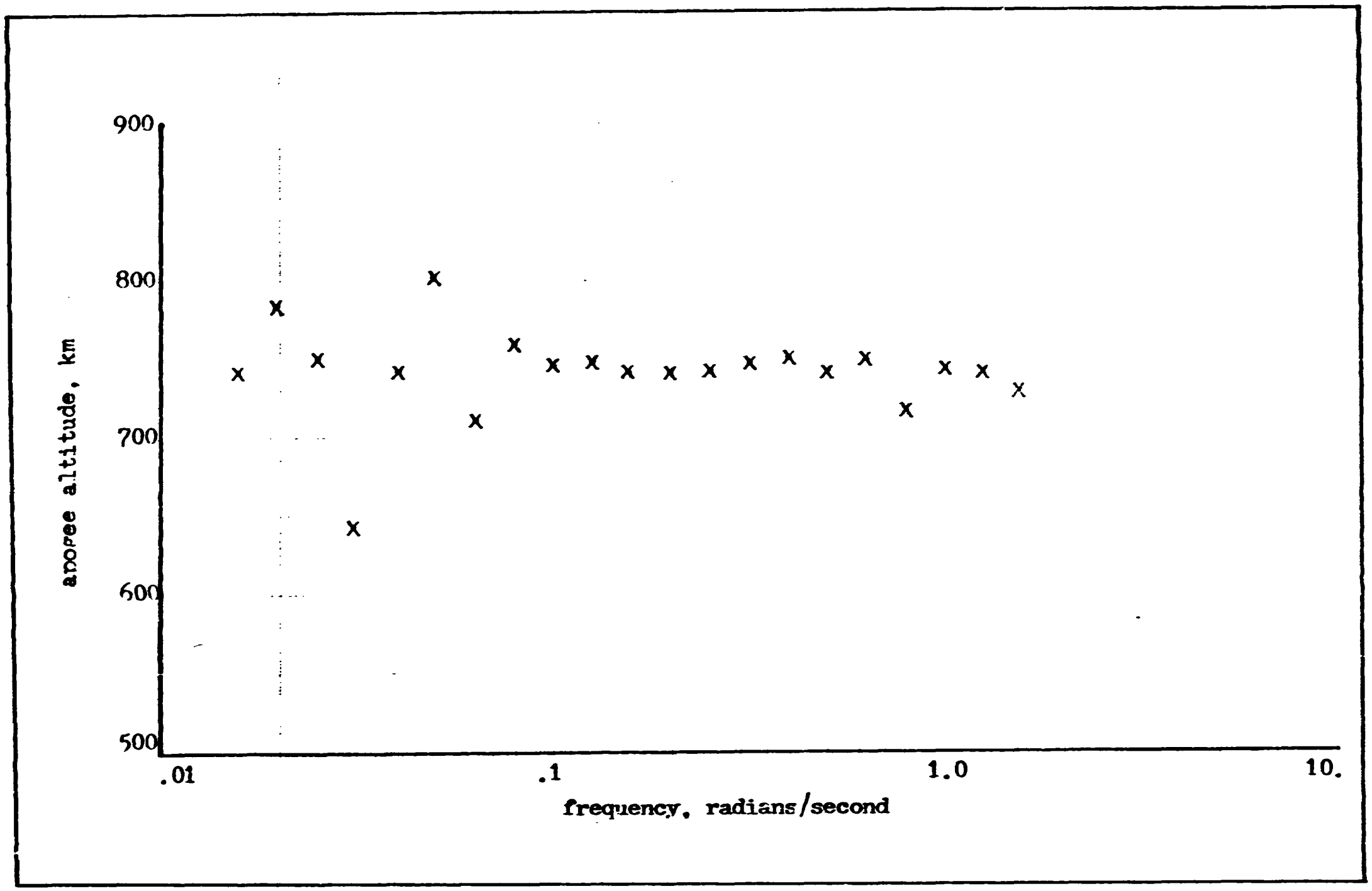

Fig. 10. Sinusoidal Flight Path Angle Error (amplitude = .004 radians)

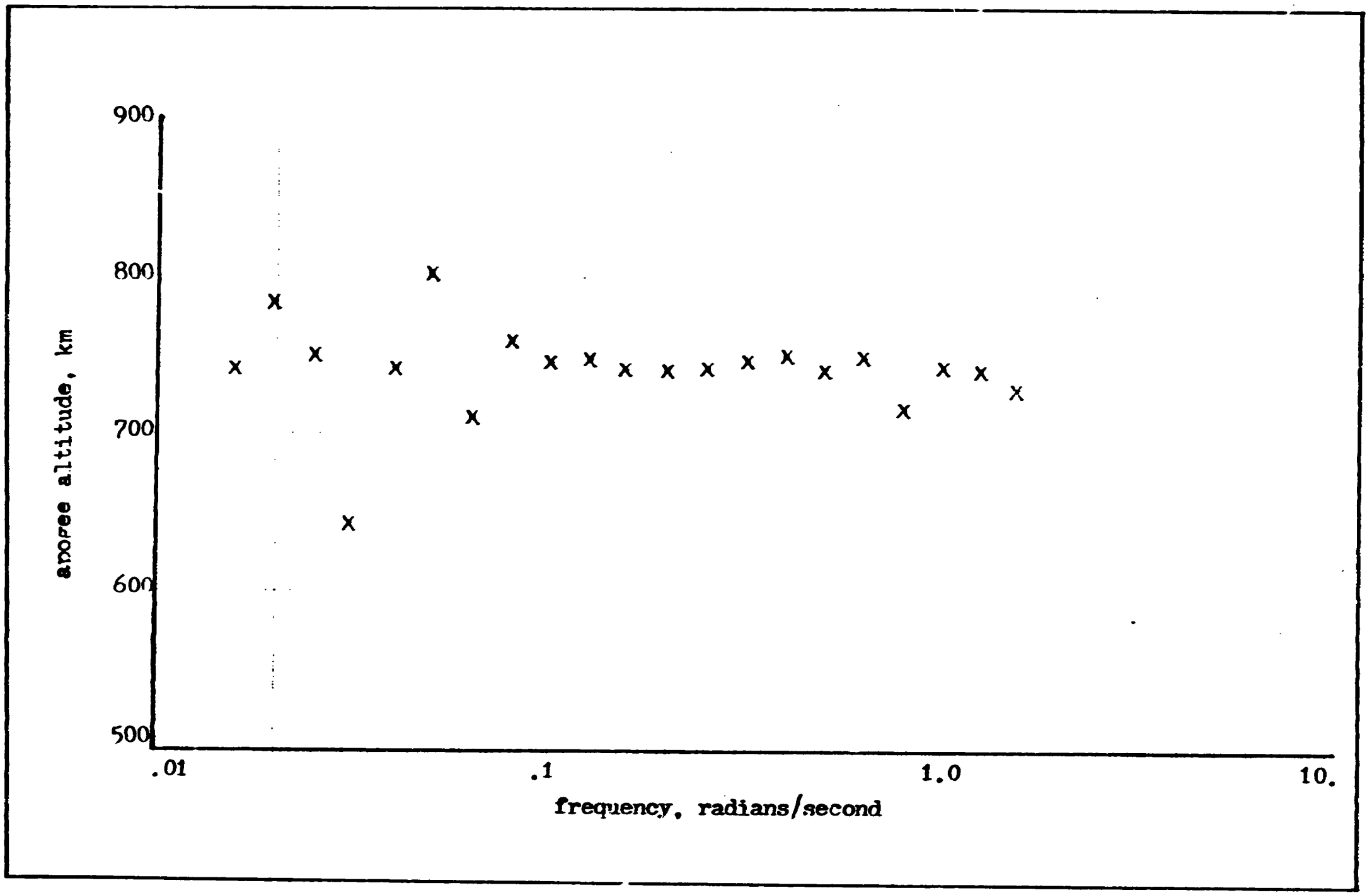

Fig. 10. Sinusoidal Flight Path Angle Error (amplitude = .004 radians)

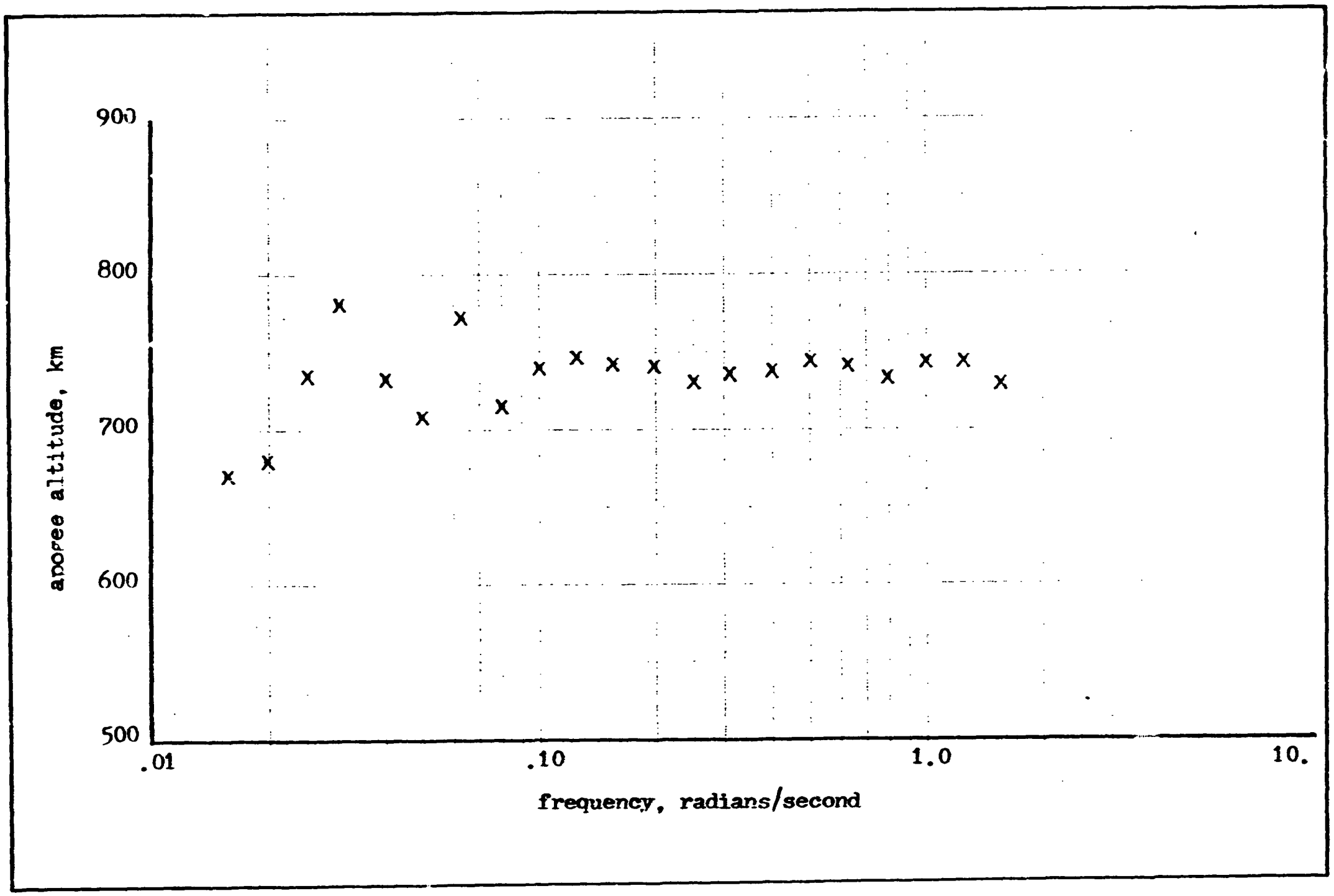

Fig. 11. Sinusoidal Acceleration Error (amplitude = .4 m/sec^2)

control effectiveness). The high frequency errors tend to cancel each other out, but at the lower frequencies there is a larger error in the sensitive region that is not cancelled out. The net effect is that the system, like most physical systems, acts like a low-pass filter. The guidance scheme did not show any instability in the frequency range examined.

The results using the off-nominal density conditions (-35%, +40%) were the same, with the data points being shifted up or down as in the constant error cases. Varying the amplitude of the errors only changed the deviation from the nominal 730 km apogee, but did not alter the shape of the figures.

Random Error

Randomly generated errors in navigational information were investigated to determine if there was a significant difference from the results obtained with constant and time-varying sinusoidal errors. It was also desired to find out if the correlation time effected the results appreciably. Correlation time, it will be recalled from the previous chapter, is the spacing between the randomly generated error parameters. Accordingly, the program was modified to run 10 randomly generated velocity error profiles (uniformly distributed between $\pm$ 20 m/sec) at each of 10 correlation times. The results are shown in Fig. 12. The correlation time is plotted versus the arithmetic mean and the standard deviation of the apogee deviations from 730 km for the 10 trajectories.

It can be seen that the standard deviation of random error is less than the apogee deviation due to constant errors, again

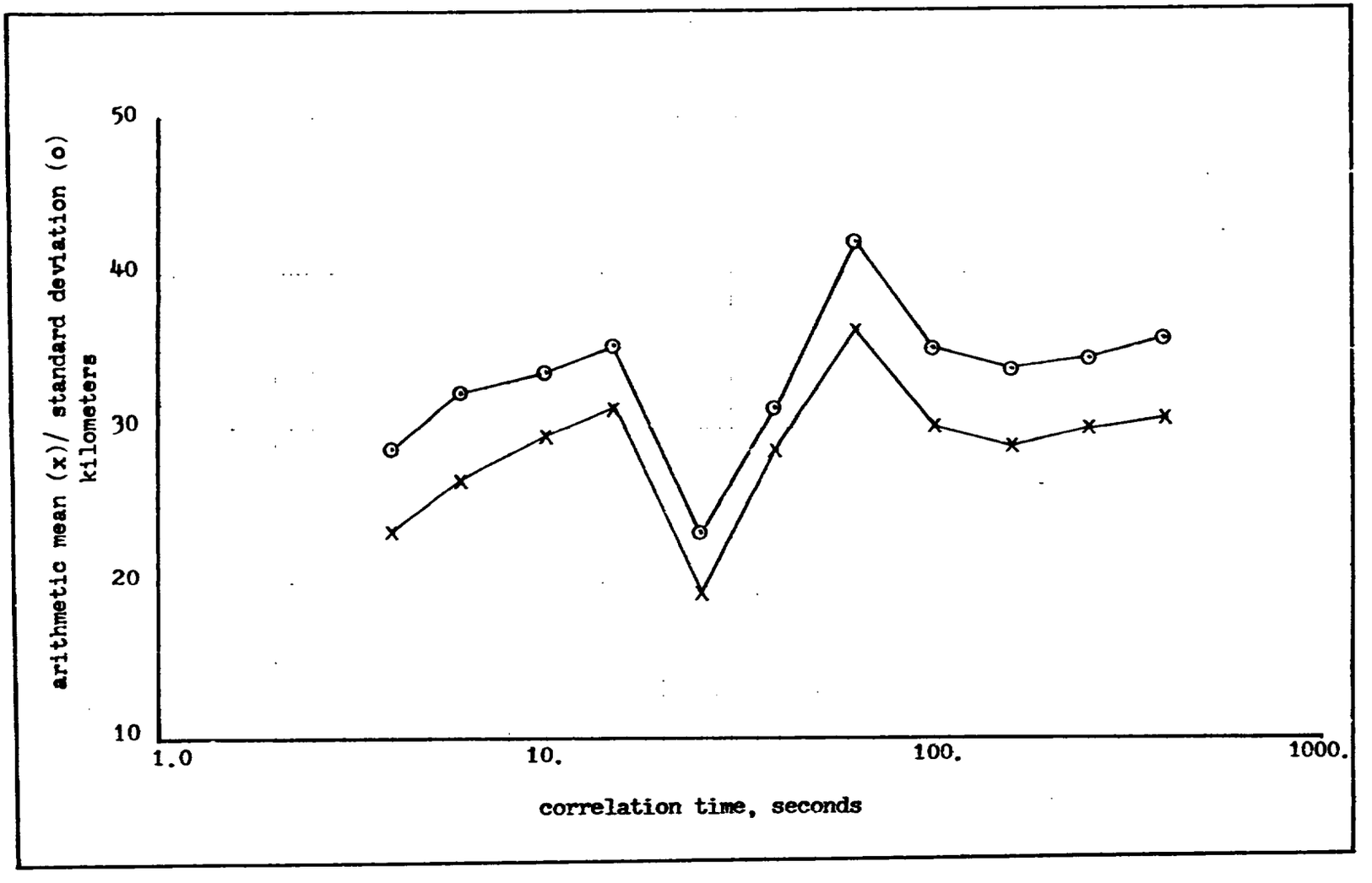

Fig. 12. Random Velocity Errors

indicating that plus and minus errors tend to cancel each other out. As might be expected, the random errors produce greater apogee deviations than the sinusoidal errors.

The relationship of correlation time to the standard deviation is ambiguous. Although the standard deviation seems to increase with correlation time (as did the apogee deviations with increasing period length in the sinusoidal case), there is a minimum at 25 seconds. At any rate, there does not seem to be a strong relationship between correlation time and apogee error.

Error Coupling

So far, in the course of this study, errors in velocity, flight path angle, and acceleration have been input singly to the simulation. It was desired to determine if it would be possible to input combinations of the error parameters and predict the apogee deviation. Using the principle of superposition, it would be possible to determine the deviation for each individual error, then sum them to find the total apogee deviation. Unfortunately, this did not prove to be the case. The results of several tests indicate that the errors are strongly coupled and superposition does not hold. This can be seen from the sample trajectory of Appendix C. Constant errors of -10 m/sec, .002 radians, and .1 m/sec^2 were input to the simulation. From Figures 6, 7, and 8, it can be determined that the apogee deviations for each case are, respectively, +40 km, -15 km, and +12 km, totaling +37 km apogee error. However, the actual apogee altitude is 727 km, or -3 km error. No further investigation of the error coupling was attempted, although the interrelationship of error parameters can be seen from the partial derivatives of eq. (20).

VI. Conclusions and Recommendations

Conclusions

This study has shown to what accuracy the AMOOS vehicle navigation system must provide velocity, flight path angle, and acceleration information to successfully implement the guidance scheme. This information can be used to select and design the navigation sensors for the vehicle.

Velocity information must be supplied to an accuracy of ±22 m/sec. Constant errors in velocity relate to apogee deviations according to the sensitivity coefficient of -4.25 km/m/sec. Flight path angle information must be supplied within the accuracy range of -.26 deg to +.20 deg. Errors in measuring acceleration along the flight path (which is used to determine atmospheric density and then a density altitude) must be within ± .6 m/sec^2. Errors in apogee altitude are related to errors in sensing acceleration by the approximate sensitivity coefficient of 120 km/m/sec^2.

These accuracy tolerances do not seem to be severe in view of the present capability of space navigation systems. The exoatmospheric navigation problem imposes more stringent accuracy requirements on navigational hardware, so there should not be a major problem in obtaining the accuracy required for the atmospheric flight.

The guidance scheme has demonstrated its capability to handle time-varying errors, both sinusoidal and random. There is no frequency instability in the guidance equations, and the apogee deviations for error frequencies above .1 rad/sec are minimal.

Recommendations

The next step in designing the navigation and guidance system for the AMOOS vehicle would be to select navigational sensors which can provide the required accuracy, both for the exoatmospheric and the atmospheric phases of the mission. Information from these sensors would have to be processed by the navigation computer before being input to the guidance system.

Existing hardware would have to be evaluated to determine if it would be suitable for use on the vehicle, or if new hardware would have to be designed.

Bibliography

1. White, John. Feasibility and Tradeoff Study of an Aeromaneuvering Orbit-to-Orbit Shuttle (AMOOS). Lockheed Missiles & Space Company, Huntsville, Alabama, July 1974. N74-32325.

2. -----. Applications Study of Aeromaneuvering Orbit-to-Orbit Shuttle (AMOOS). Lockheed Missiles & Space Company, Huntsville, Alabama, January 1976. N76-18210.

3. U.S. Standard Atmosphere, 1962. Washington, D.C.: U.S. Government Printing Office, 1962.

4. Space Tug Aerobraking Astrionic System Study. IBM Report Number 72W-00070. International Business Machines Corporation, Huntsville, Alabama, October 1971.

5. Kirk, Donald E. Optimal Control Theory. Englewood Cliffs, New Jersey: Prentice-Hall, Inc., 1970.

APPENDIX A

The AMOOS Concept

The Aeromaneuvering Orbit-to-Orbit Shuttle (AMOOS) is designed to be carried to and from low earth orbit inside the Shuttle Orbiter payload bay. Basically, AMOOS differs from the Space Tug in that it returns to low earth orbit by making a braking pass through the atmosphere. The added vehicle weight due to increased structural strength and the addition of a thermal protection system is more than offset by the weight of fuel required for the same propulsive braking. Thus, AMOOS can carry 2 to 3 times the payload to GEO for the same weight vehicle.

The AMOOS concept has been proposed for both manned and unmanned missions. The mission of primary interest is to geosynchronous altitude, and that is the mission profile examined in this study. However, the concept is not limited to high earth orbits. An AMOOS vehicle could be used upon returning to earth from lunar missions, or it could be used to provide aeromaneuvering in any planetary atmosphere.

In order to provide for the maximum efficient use of the Shuttle, AMOOS is sized to the maximum Shuttle payload weight. The dimensions of the payload bay require that AMOOS be shaped like a cylinder with one end modified to an aerodynamic nose cap. The general configuration is shown in Fig. 13.

The nose cap is hinged to permit the rocket engine to fire forward. This aft cargo bay arrangement permits the vehicle to be adapted to modular configuration. A hinged flap at the rear provides the

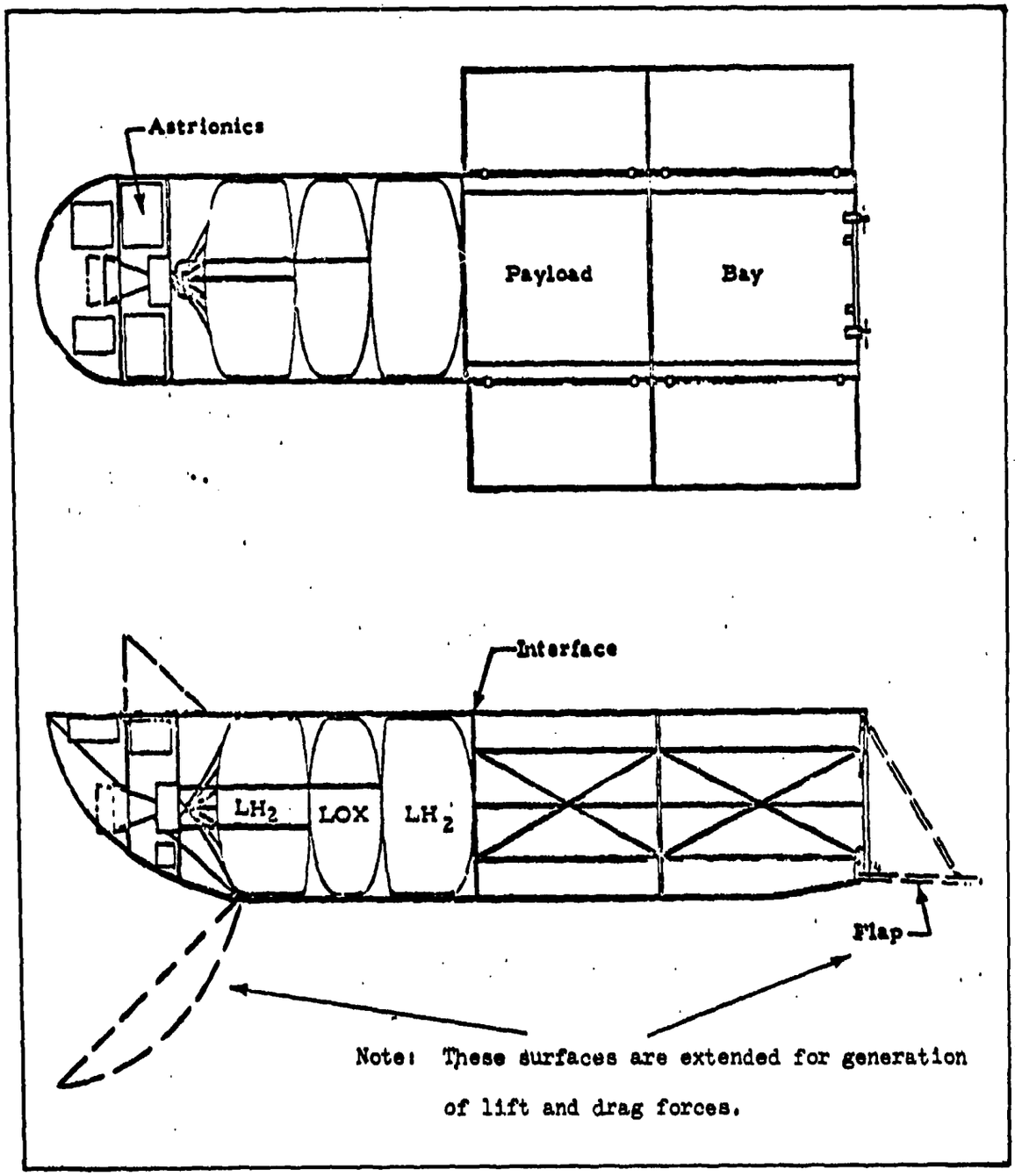

Fig. 13. General Configuration of the AMOOS vehicle (Ref 1:155)

required aerodynamic trim characteristics. An ablative thermal protection system is used on the vehicle, and it must be replaced after each mission.

The possibility exists of placing heavy payloads into GEO by staging 2 AMOOS vehicles (using 2 Shuttle flights). This would permit the placing of a 15,000 kg payload into GEO. A single stage AMOOS can carry a round trip payload of 2860 kg, or deliver 5200 kg. This compares to 1100 kg and 3600 kg, respectively, for the all-propulsive Space Tug. Thus it can be seen that AMOOS enjoys a definite performance advantage over the Space Tug.

Estimated costs (Ref 1:54) for the design, developement, testing, evaluation, and production of AMOOS are as follows (in 1970 United States dollars):

DDT&E	511. million
1st unit production	28.7 million
refurbishment (per flight)	1.1 million

These estimates do not include engine costs, estimated at $130 million for DDT&E, and $.7 million unit cost; facility and operations costs; and the prime contractor's fee.

Figure 14 shows the orientation of the vehicle with respect to angle of attack (α), bank angle (β), and flight path angle (γ). Note that bank angle, as defined, is not the angle produced by a simple roll about the vehicle centerline. The autopilot must orient the vehicle to change the direction of the lift vector by angle β while keeping the lift vector, vehicle centerline, and the relative wind vector in the same plane. This allows the vehicle to keep the same side (covered with ablative material) flying into the relative wind.

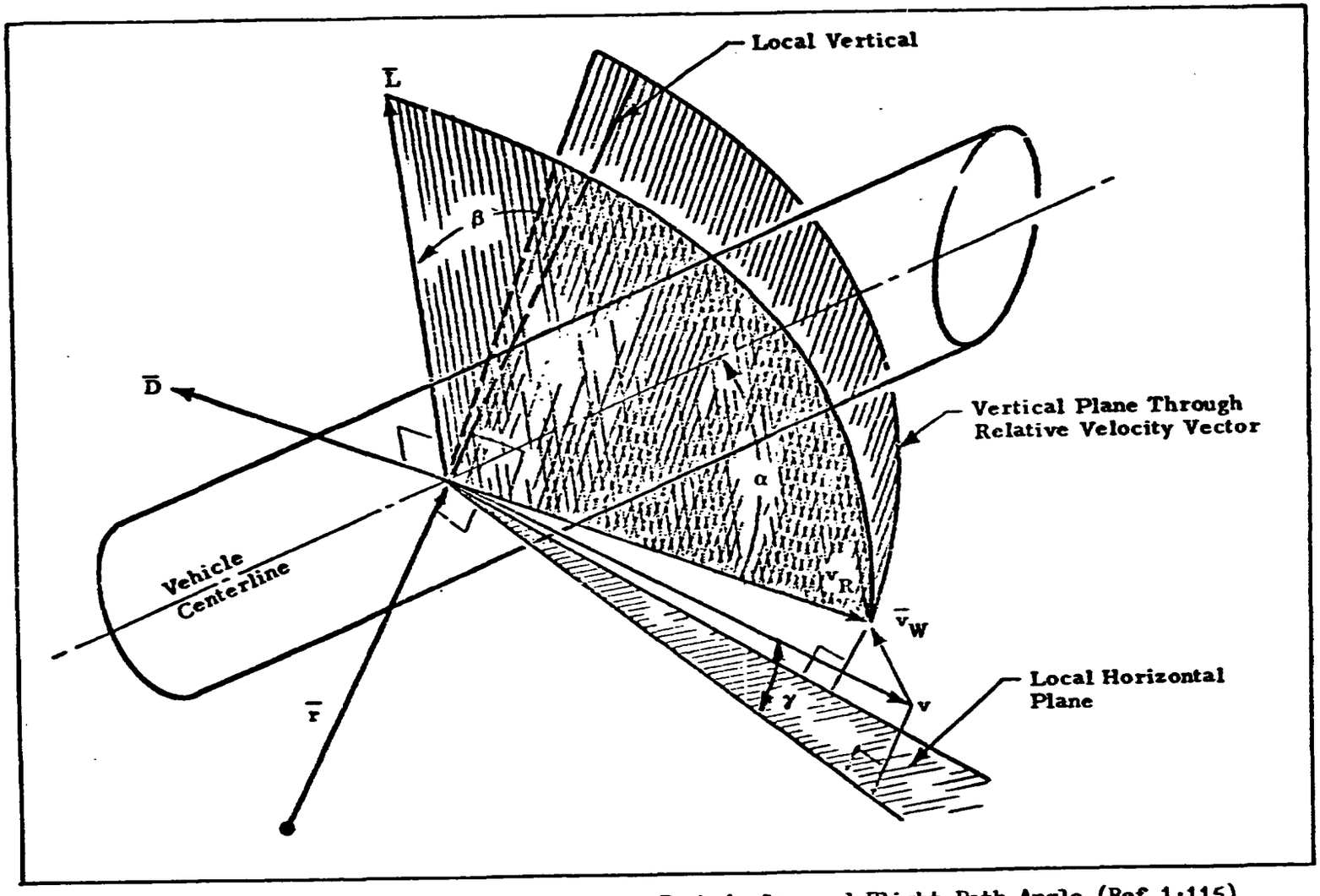

Fig. 14. Definition of Angle of Attack, Bank Angle, and Flight Path Angle (Ref 1:115)

APPENDIX B

Program Listing

The computer listing which follows was used to simulate the vehicle trajectories. The program uses the following input information:

1. ERRVEL - velocity error = in this example, -10 m/sec constant error
2. ERRGAM - flight path angle error = in this example, +.002 radians constant error
3. ERRACC - acceleration error = in this example, +.1 m/sec^2 constant error
4. IFOR - format parameter = 0 for short output, 1 for full output
5. ITRAJ - trajectory designator = in this example, #1
6. VAP - vacuum perigee = 71.1133 km
7. DX - guidance cycle time = 4 sec
8. DT - simulation time step = 1 sec
9. $C_i(t)$ - feedback gain vector (see Fig. 4)

The output from this program is given in Appendix C.

```
      PROGRAM TH 31(INPUT,OUTPUT)
C     NAVIGATION AND GUIDANCE SIMULATION PROGRAM FOR AN
C     MANEUVERING SPACE VEHICLE
      COMMON /RO/V,VI,RHO,CD,CL,AR,M,MJ,GAMMA,R,BETAO,U,VR(3),UD(3),
     *UL(3),L,ACCEL
      DIMENSION Y( ),RI(3),VI(3),VVE(3),WIE(3),B(3),S(6),HV(3),
     *IC(3),JC(3),TGO(100),C1(100),C2(100),C3(100),D(6)
      DIMENSION A(11),ANOM(500),VNOM(500),GNOM(500),TIME(500)
      DIMENSION EM(1000)
      REAL M,MU,MI,INC,MAG
      ALL L=-10.
      DEGAM=.002
      DRACC=.1
      MA=.
      N=3    $   TMAX=600.
      RHOFAC=1.
      IE  =0
      DTR=.017453293    $    RTD=57.29577951
      WIE=7.2921152E-5    $    MU=3.986032E14   $    RE=6378165.
      H=  ..    $   CD=2.3125    $    CL=1.3457    $    AR=15.69
        =1.
      I=0    $    J=0
      L=0    $    IG=0
      W  (1)=0    $    WIE(2)=0    $    WIE(3)=WE
        TOP,IEOP,ITRAJ,VAR,DX,DT
      VAR=VAR*1000.+R
      RHOO=1.2250    $    BETAO=90.*DTR
      ALTAMAX=70.*DTR
      AI=1.235    $    RSYNCH=35786767.
      AT=  +AI
      E=-MU/(VRR+RSYNCH)
      VVR=SQRT(2.*(MU/VRR+E))
      H=VRR*VVR
      V=SQRT(2.*(MU/RI+E))
      GAMMA=-ACOS(H/(RI*V))
      GD=GAMMA*RTD
```

```
C *******   THIS SECTION GENERATES A NOMINAL TRAJECTORY                    0037
      HP=(RP-RE)/1000.                                                    0038
      PRINT 10,ITRAJ,V,GD,VRPK,DX,DT                                      0039
   10 FORMAT(///" TRAJECTORY # ",I2,/" ENTRY CONDITIONS (120 KM)"         0040
     +/" INITIAL VELOCITY, M/SEC = ",F10.2,/" FLIGHT PATH ANGLE (GAMMA)  0041
     +, DEG = ",F10.3,/" VACUUM PERIGEE, KM = ",F10.4,/" GUIDANCE CYCLE  0042
     +TIME, SEC = ",F5.2,/" SIMULATION TIME STEP, SEC = ",F5.2)           0043
      X=0    $    R=RI                                                    0044
      IF(IFOR.LT.1) GO TO 15                                              0045
      PRINT 15                                                            0046
   15 FORMAT(//"TIME",T15,"GAMMA",T24,"VELOCITY",T39,"ALTITUDE",T55,      0047
     +"DENSITY"/)                                                         0048
   16 CONTINUE                                                            0049
      Y(1)=V    $    Y(2)=GAMMA    $    Y(3)=R                           0050
      CALL F(X,Y,P)                                                       0051
   20 J=J+1    $    Z=(R-RE)/1000.                                        0052
      RHO=RHOO*EXP(-Z/7.715)                                              0053
   22 W=.5*RHO*V**2                                                       0054
      CALL PRDES(X,Y,N,DX)                                                0055
      V=Y(1)    $    GAMMA=Y(2)    $    R=Y(3)                          0056
      TIME(J)=X    $    VMOM(J)=V    $    GMOM(J)=GAMMA                  0057
      ALOM(J)=R-RE                                                        0058
      GD=GMOM(J)*RTD                                                      0059
      IF(IFOR.LT.1) GO TO 21                                              0060
      PRINT 30,TIME(J),GD,VMOM(J),ALOM(J),RHO                             0061
   30 FORMAT(F7.2,F12.4,F12.2,E15.6,F15.6)                                0062
   21 CONTINUE                                                            0063
      IF((R-RE).GT.92000..AND.GAMMA.LT.0) TDELAY=X                        0064
      IF((R-RE).LE.0.)STOP"VEHICLE HAS REENTERED"                         0065
      IF(Y.LE.YMAX.AND.R-RE.LT.1.E5) GO TO 20                             0066
      YMAX=Y    $    J=0                                                  0067
      H=R*V*COS(GAMMA)                                                    0068
      E=V**2/2.-MU/R                                                      0069
      SA=-MU/(2.*E)*(1.+SQRT(1.+2.*E*H**2/MU**2))                         0070
      APOGEE=(SA-RE)/1000.                                                0071
      TFIN=X                                                              0072
```

```
      PRINT 35,APOGEE,TDELAY                                            0073
   35 FORMAT(/" TARGET APOGEE ALTITUDE = ",F10.2,/                      0074
     +" TIME DELAY = ",F9.1,/)                                          0075
      PRINT 40                                                          0076
   40 FORMAT(T5,"TABLE OF GUIDANCE CONSTANTS"/" TIME",T15,"C1",T26,"C2" 0077
     +,T36,"C3")                                                        0078
      READ,NGC                                                          0079
      DO 50 I=1,NGC                                                     0080
      READ,TGC(I),C1(I),C2(I),C3(I)                                     0081
      PRINT 45,TGC(I),C1(I),C2(I),C3(I)                                 0082
   45 FORMAT(F8.1,F10.4,F10.1,F10.6)                                    0083
   50 CONTINUE                                                          0084
C  ********   THIS SECTION COMPUTES INERTIAL INITIAL CONDITIONS         0085
      SMA=(VR2+RSYMCH)/2.                                               0086
      ECC=(SMA-VR2)/SMA                                                 0087
      INC=21.5*RTD                                                      0088
      P=VR2*(1.+ECC)                                                    0089
      NU=-ACOS((P/RI-1.)/ECC)                                           0090
      RR1=RI*COS(NU)                                                    0091
      RR2=RI*SIN(NU)                                                    0092
      VR1=SQRT(MU/P)*SIN(NU)                                            0093
      VR2=SQRT(MU/P)*(ECC+COS(NU))                                      0094
      R(1)=RR1                                                          0095
      R(2)=COS(INC)*RR2                                                 0096
      R(3)=-SIN(INC)*RR2                                                0097
      V(1)=VR1                                                          0098
      V(2)=COS(INC)*VR2                                                 0099
      V(3)=-SIN(INC)*VR2                                                0100
      DINC=INC*RTD    $     DNU=NU*RTD                                 0101
      PRINT*                                                            0102
      PRINT*,"TRANSFER ORBIT ELEMENTS"                                  0103
      PRINT*,"INCLINATION = ",DINC," DEG"                               0104
      PRINT*,"ECCENTRICITY = ",ECC                                      0105
      PRINT*,"TRUE ANOMALY AT ENTRY = ",DNU," DEG"                      0106
      PRINT*                                                            0107
      PRINT*,"INERTIAL POSITION AND VELOCITY AT ENTRY"                  0108
```

```
      PRINT*,"P(I) = ", P(1)," METERS"                                  0109
      PRINT*,"P(J) = ", P(2)," METERS"                                  0110
      PRINT*,"P(K) = ", P(3)," METERS"                                  0111
      PRINT*,"V(I) = ", P(4)," METERS/SEC"                              0112
      PRINT*,"V(J) = ", P(5)," METERS/SEC"                              0113
      PRINT*,"V(K) = ", P(6)," METERS/SEC"                              0114
      PRINT*                                                            0115
C     CONTINUE                                                          0116
C     ********  THIS SECTION GENERATES A RANDOM SEQUENCE               0117
C     CONTINUE                                                          0118
      CALL RANSET(SEED)                                                 0119
      DO 51 I=1,300,NR                                                  0120
   51   R(I)=(RANF(0)-.5)*2.                                            0121
      DO 52 I=1,200,NR                                                  0122
      RM=NR-1                                                           0123
      DO 52 J=1,NRM                                                     0124
   52 RM(I+J)=(RM(I+NR)-RM(I))*J/(FLOAT(NR))+RM(I)                      0125
C     CONTINUE                                                          0126
      PRINT*                                                            0127
      PRINT*                                                            0128
      PRINT*                                                            0129
      PRINT*,"VELOCITY ERROR = ",ERRVEL                                 0130
      PRINT*,"FLIGHT PATH ANGLE ERROR = ",ERRGAM                        0131
      PRINT*,"MEASURED DECELLERATION ERROR = ",ERRACC                   0132
      L=1    $   M=2    $   IR=-1                                       0133
      P(1)=P(1)    $   P(2)=P(2)    $   P(3)=P(3)                      0134
      V(4)=P(4)    $   V(5)=P(5)    $   V(6)=P(6)                      0135
      P1(1)=P(1)    $   P1(2)=P(2)    $   P1(3)=P(3)                   0136
      V1(1)=P(4)    $   V1(2)=P(5)    $   V1(3)=P(6)                   0137
      T=0                                                               0138
      RHOV=2400*RHOERR                                                  0139
      BETAC=30.*DTR                                                     0140
      BETAJ=31.*DTR                                                     0141
      BETA=BETAC*DTR                                                    0142
      ALT=MAG(P1)-RE                                                    0143
      Z=ALT/1000.                                                       0144
```

```
      IF(IFOR.LT.1) GO TO 100                                                   0145
      PRINT 75                                                                  0146
   75 FORMAT(//,T40,"ACTUAL VEHICLE TRAJECTORY"//" TIME",T15,"ALTITUDE",0147
     +T27,"VELOCITY",T42,"GAMMA",T55,"DENSITY",T65,"BETA COMMAND",          0148
     +T81,"INCLINATION"/" (SECONDS)",T15,"(METERS)",T27,"(M/SEC)",          0149
     +T42,"(DEGREES)",T55,"(KG/M3)",T65,"(DEGREES)",T81,"(DEGREES)")        0150
C********   THIS SECTION SIMULATES THE VEHICLE TRAJECTORY                    0151
  100 CONTINUE                                                              0152
      RHO=.01*EXP(-Z/7.217)                                                 0153
      CALL CROSS(V1,WE,R1)                                                  0154
      VR(1)=V1(1)-VVE(1)    $   VR(2)=V1(2)-VVE(2)    $   VR(3)=V1(3)     0155
     +-VV(3)                                                                0156
      UD(1)=-VR(1)/MAG(VR)    $   UD(2)=-VR(2)/MAG(VR)    $   UD(3)=-VR(3)0157
     +/MAG(VR)                                                              0158
      CALL CROSS(R1,V1,HV)                                                  0159
      CALL CROSS(HV,R1,H)                                                   0160
      UL(1)=UL(1)*COS(BETA)/(MAG(VR)**2*MAG(R1))                            0161
     +-R(1)*SIN(BETA)/(MAG(R1)*MAG(VR))                                     0162
      UL(2)=UL(2)*COS(BETA)/(MAG(VR)**2*MAG(R1))                            0163
     +- (2)*SIN(BETA)/(MAG(R1)*MAG(VR))                                     0164
      UL(3)=UL(3)*COS(BETA)/(MAG(VR)**2*MAG(R1))                            0165
     +-V(3)*SIN(BETA)/(MAG(R1)*MAG(VR))                                     0166
      UL=MAG(UL)                                                            0167
      CALL RKQS(T,S,H,DT)                                                   0168
      R1(1)=S(1)    $   R1(2)=S(2)    $   R1(3)=S(3)                      0169
      V1(1)=S(4)    $   V1(2)=S(5)    $   V1(3)=S(6)                      0170
      IF(T.GT.TMAX) STOP "MAXIMUM TIME EXCEEDED"                            0171
      IF(MAG(R1).LT.(RE+5.E3) STOP "VEHICLE HAS REENTERED"                  0172
      IF(MAG(R1).GT.RE+1.E5.AND.GAMMA.GT.0) GO TO 600                       0173
      ALT=MAG(R1)-RE                                                        0174
      T=SLT/1000.                                                           0175
      VEL=MAG(V1)                                                           0176
      CALL CROSS(HV,R1,V1)                                                  0177
      H=MAG(HV)                                                             0178
      INC=ACOS(HV(3)/H)*RTD                                                 0179
      GAMMA=ACOS(H/(MAG(R1)*MAG(V1)))                                       0180
```

```
      GAMMA=SIGN(GAMMA,R1(1)*V1(1)+R1(2)*V1(2)+R1(3)*V1(3))
      GD=GAMMA*RTD
C*******   THIS SECTION SIMULATES THE NAVIGATION SYSTEM ERROR
      RC(1)=R1(1)    $    RC(2)=R1(2)    $    RC(3)=R1(3)
      VC(1)=V1(1)    $    VC(2)=V1(2)    $    VC(3)=V1(3)
      VCM=MAG(VC)+ERRVEL*RM(IT)
      GAMMA=GAMMA+ERRGAM*RM(IT)
      ACCM=ACCEL+ERRACC*RM(IT)
      IF(ACCM.LT.0) ACCM=.0001
C*******   THIS SECTION SIMULATES THE GUIDANCE SYSTEM
      IG=IG+1
      IF(IG.LT.DX) GO TO 400
      IG=0
      IF(T.GT.TFIN) GO TO 400
      IT=IFIX(T/DX)
      IT=IT-IDELAY
      RHO=2.*ACCM*M/(((MAG(V2)+ERRVEL)**2)*CD*AR)
      ALT=-7315.*ALOG(RHO/RHOO)
      TC1=TRLNDC(1,2,C1,TGC,31,GT)
      TC2=TRLNDC(1,2,C2,TGC,31,GT)
      TC3=TRLNDC(1,2,C3,TGC,31,GT)
      U=TC1*(VCM-VNOM(IT))+TC2*(GAMMA-GNOM(IT))+TC3*(ACM-ANOM(IT))
      IF(U.GT.1.345) U=1.345699
      IF(U.LT.-1.345) U=-1.345699
      BETAD=ACOS(U/CL+COS(BETAO))
      IF(BETAD-BETAO.GT.BETAMAX) BETAD=BETAO+BETAMAX
      IF(BETAO-BETAD.GT.BETAMAX) BETAD=BETAO-BETAMAX
      BDD=BETAD*RTD
      IF(IPR.LT.1) GO TO 400
      PRINT 150,T,ALT,VEL,GD,RHO,BDD,DINC
 150  FORMAT(/,F7.2,F15.1,F12.2,F12.4,E15.6,F15.1,F15.4)
C*******   THIS SECTION SIMULATES THE AUTOPILOT
 400  BETA=BETAD
      BD=BETA*RTD
      GO TO 100
 500  CALL ORBS(HV,R1,V1)
```

```
      =MAG(V1)**2/2.-MU/MAG(R1)                                          0217
      PE=-MU*(2.*E)*(1.+SQRT(1.+2.*E*MAG(HV)**2/MU**2))                  0218
      PROG=(RM-RE)/1000.                                                 0219
      PRINT*                                                             0220
      PRINT*,"DENSITY VARIATION = ",RHOFAC                               0221
      PRINT*,"ACTUAL APOGEE ALTITUDE = ",APOGEE," KM"                    0222
      PRINT *                                                            0223
      END                                                                0224
      SUBROUTINE F(X,Y,P)                                                0225
      COMMON /RC/V,VI,RHO,CD,CL,AR,M,MU,GAMMA,R,BETAO,U,VR(3),UD(3),     0226
     +UL(3),L,ACCEL                                                      0227
      DIMENSION Y(6),P(6)                                                0228
      REAL M,MU,MAG                                                      0229
      IF(L-1)500,520,520                                                 0230
  500 P(1)=-(Y(1)-VC)**2*RHO*CD*AR/(2.*M)-MU*SIN(Y(2))/Y(3)**2           0231
      P(2)=(Y(1)-VC)**2*AR*RHO*(CL*COS(BETAO)+U)/(2.*M*Y(1))             0232
     +-(MU/(Y(1)*Y(3)**2)-Y(1)/Y(3))*COS(Y(2))                           0233
      P(3)=Y(1)*SIN(Y(2))                                                0234
      GO TO 550                                                          0235
  520 P(1)=Y(4)                                                          0236
      P(2)=Y(5)                                                          0237
      P(3)=Y(6)                                                          0238
      P(4)=-MU*Y(1)/(Y(1)**2+Y(2)**2+Y(3)**2)**1.5+RHO*(MAG(VR)**2)      0239
     +*AR*CL*UL(1)/(2.*M)+RHO*(MAG(VR)**2)*AR*CD*UD(1)/(2.*M)            0240
      P(5)=-MU*Y(2)/(Y(1)**2+Y(2)**2+Y(3)**2)**1.5+RHO*(MAG(VR)**2)      0241
     +*AR*CL*UL(2)/(2.*M)+RHO*(MAG(VR)**2)*AR*CD*UD(2)/(2.*M)            0242
      P(6)=-MU*Y(3)/(Y(1)**2+Y(2)**2+Y(3)**2)**1.5+RHO*(MAG(VR)**2)      0243
     +*AR*CL*UL(3)/(2.*M)+RHO*(MAG(VR)**2)*AR*CD*UD(3)/(2.*M)            0244
      ACCEL=RHO*(MAG(VR)**2)*AR*CD/(2.*M)                                0245
  550 RETURN                                                             0246
      END                                                                0247
      REAL FUNCTION MAG(A)                                               0248
      DIMENSION A(3)                                                     0249
      MAG=SQRT((A(1)**2)+(A(2)**2)+(A(3)**2))                            0250
      RETURN                                                             0251
      END                                                                0252
```

```
0253
0254
0255
0255
0257
0258
0259
```

APPENDIX C

Sample Trajectory

The sample trajectory contained in this section was produced by the program listed in Appendix B.

The output consists of the following:

1. Echo print of input data, plus calculated entry conditions.
2. Nominal trajectory which the guidance system will try to control the vehicle along. Total time of flight is 420 seconds, and perigee (when flight path angle changes from - to +) is 70.113 km.
3. Desired apogee altitude and time required to descend to 95.4 km.
4. Echo print of feedback gain vector.
5. Transfer orbit elements and inertial position and velocity at beginning of atmospheric phase of flight.
6. Echo print of error inputs.
7. Actual vehicle trajectory, giving actual altitude, velocity, and flight path angle; calculated density; commanded bank angle; and inclination of the osculating orbit.
8. Density profile which was used in this trajectory, and the actual apogee altitude the vehicle reached.

TRAJECTORY # 1
ENTRY CONDITIONS (120 KM)
INERTIAL VELOCITY, M/SEC = 10183.52
FLIGHT PATH ANGLE (GAMMA), DEG = -4.503522
VACUUM PERIGEE, KM = 71.1133
GUIDANCE CYCLE TIME, SEC = 4.00
SIMULATION TIME STEP, SEC = 1.00

TIME	GAMMA	VELOCITY	ALTITUDE	DENSITY
4.00	-4.755300	10191.77	.116352E+06	.919739E-07
8.00	-4.219127	10194.00	.113835E+06	.141474E-06
12.00	-4.053211	10195.40	.110365E+06	.214432E-06
16.00	-3.915164	10198.77	.108025E+06	.320575E-06
20.00	-3.763990	10210.70	.105232E+06	.472577E-06
24.00	-3.621732	10212.48	.102562E+06	.655300E-06
28.00	-3.474384	10233.74	.100136E+06	.934194E-06
32.00	-3.325953	10224.45	.977153E+05	.138993E-05
36.00	-3.173554	10206.45	.953933E+05	.133725E-05
40.00	-3.022171	10203.53	.931974E+05	.265622E-05
44.00	-2.854361	10201.57	.919811E+05	.359335E-05
48.00	-2.727707	10195.13	.898901E+05	.479307E-05
52.00	-2.590799	10192.33	.871544E+05	.639141E-05
56.00	-2.444246	10181.18	.853942E+05	.816315E-05
60.00	-2.293184	10175.66	.837033E+05	.104292E-04
64.00	-2.152772	10152.69	.821233E+05	.131394E-04
68.00	-2.003197	10146.20	.805593E+05	.162051E-04
72.00	-1.856675	10125.71	.792453E+05	.199342E-04
76.00	-1.722447	10130.75	.780133E+05	.240400E-04
80.00	-1.581784	10070.03	.768562E+05	.285925E-04
84.00	-1.442975	10035.94	.757959E+05	.335182E-04
88.00	-1.305330	9937.75	.748349E+05	.387400E-04
92.00	-1.172169	9943.70	.739714E+05	.441733E-04
96.00	-1.040312	9894.45	.732044E+05	.497191E-04
100.00	-.912580	9842.22	.725321E+05	.551933E-04
104.00	-.787777	9780.78	.719493E+05	.605153E-04
108.00	-.665687	9715.25	.714552E+05	.655299E-04
112.00	-.543564	9646.93	.710444E+05	.701151E-04

116.00	-.435628	9573.73	.707173E+05	.741553E-04
120.00	-.330859	9439.41	.704594E+05	.775343E-04
124.00	-.227993	9423.55	.702773E+05	.903393E-04
128.00	-.124523	9347.11	.701534E+05	.623551E-04
132.00	-.023098	9270.72	.701135E+05	.935534E-04
136.00	.051476	9194.76	.701236E+05	.542310E-04
140.00	.143939	9120.34	.701993E+05	.541145E-04
144.00	.227033	9047.76	.703953E+05	.533359E-04
148.00	.303536	8977.17	.704754E+05	.920170E-04
152.00	.373809	8909.40	.706877E+05	.591544E-04
156.00	.443854	8847.04	.709413E+05	.775714E-04
160.00	.507886	8783.36	.712343E+05	.752120E-04
164.00	.559987	8724.59	.715531E+05	.722333E-04
168.00	.626530	8659.19	.719261E+05	.590315E-04
172.00	.677722	8617.77	.723132E+05	.657438E-04
176.00	.727554	8569.11	.727413E+05	.623941E-04
180.00	.774321	8523.64	.731593E+05	.596142E-04
184.00	.813217	8441.27	.736513E+05	.557129E-04
188.00	.853430	8441.59	.741574E+05	.518558E-04
192.00	.893144	8405.76	.746743E+05	.486337E-04
196.00	.934575	8371.37	.752110E+05	.451537E-04
200.00	.963774	8340.72	.757652E+05	.419794E-04
204.00	1.001920	8311.52	.763393E+05	.339324E-04
208.00	1.031428	8231.80	.769277E+05	.359565E-04
212.00	1.053140	8259.61	.775315E+05	.331371E-04
216.00	1.083294	8235.71	.781593E+05	.307371E-04
220.00	1.113015	8217.36	.787613E+05	.280754E-04
224.00	1.137423	8198.37	.794255E+05	.257525E-04
228.00	1.160627	8181.58	.800833E+05	.235737E-04
232.00	1.183730	8165.20	.807524E+05	.215542E-04
236.00	1.203926	8151.76	.814321E+05	.195714E-04
240.00	1.224004	8138.17	.821222E+05	.179261E-04
244.00	1.243344	8125.12	.828225E+05	.157119E-04
248.00	1.261929	8115.11	.835324E+05	.146225E-04
252.00	1.279380	8103.96	.842523E+05	.131513E-04
256.00	1.297965	8095.47	.849903E+05	.121312E-04
260.00	1.313719	8087.19	.857133E+05	.110754E-04
264.00	1.329867	8079.12	.864542E+05	.937722E-05

268.00	1.743539	8072.82	.872193E+05	.201999E-05
272.00	1.751770	4065.41	.879895E+05	.512773E-05
276.00	1.773525	8058.55	.887595E+05	.732704E-05
280.00	1.703115	8055.18	.895236E+05	.575124E-05
284.00	1.7 4280	8050.26	.903141E+05	.532532E-05
288.00	1.618149	8045.73	.911063E+05	.533247E-05
292.00	1.631750	8041.77	.918973E+05	.477321E-05
296.00	1.643107	8037.74	.9271 +3E+05	.428135E-05
300.00	1.654241	8034.20	.935255E+05	.333409E-05
304.00	1.671172	8030.33	.943491E+05	.347308E-05
308.00	1.687313	8027.30	.951731E+05	.396559E-05
312.00	1.695494	8025.57	.960131E+05	.277753E-05
316.00	1.703914	8022.44	.968547E+05	.244773E-05
320.00	1.721197	8019.09	.977030E+05	.217597E-05
324.00	1.733348	8017.57	.985573E+05	.133351E-05
328.00	1.745356	8015.70	.994133E+05	.172473E-05
332.00	1.757281	8013.44	.100287E+06	.157710E-05
336.00	1.751992	8011.50	.101167E+06	.136153E-05
340.00	1.759807	8009.15	.102042E+06	.129913E-05
344.00	1.792432	8007.29	.102323E+06	.197115E-05
348.00	1.773373	8005.19	.103822E+06	.943322E-05
352.00	1.615435	8004.77	.104722E+06	.639757E-05
356.00	1.573823	8003.90	.105523E+06	.7+2773E-05
360.00	1.573141	8001.40	.106543E+06	.555173E-05
364.00	1.543321	8000.01	.107453E+06	.570011E-05
368.00	1.563578	7498.78	.108382E+06	.510933E-05
372.00	1.571704	7997.18	.109312E+06	.450256E-05
376.00	1.582771	7995.91	.110248E+06	.396301E-05
380.00	1.593782	7994.46	.111193E+06	.343358E-05
384.00	1.704739	7993.13	.112173E+06	.305705E-05
388.00	1.715961	7991.32	.113093E+06	.258413E-05
392.00	1.725492	7990.73	.114053E+06	.23647+E-05
396.00	1.737292	7933.25	.115013E+06	.207733E-05
400.00	1.743343	7987.79	.115333E+06	.191735E-05
404.00	1.753746	7986.72	.116963E+06	.155129E-05
408.00	1.754401	7985.46	.117951E+06	.139222E-05
412.00	1.731008	7984.21	.118341E+06	.121733E-05
416.00	1.733559	7982.97	.119935E+06	.115315E-05
420.00	1.791983	7981.72	.120935E+06	.927352E-07

TARGET APOGEE ALTITUDE = 720.00
TIME DELAY = 40.0

TABLE OF GUIDANCE CONSTANTS

TIME	C1	C2	C3
0.0	1.0000	-65.0	-.000090
10.0	0.0700	-95.0	-.000130
20.0	0.0010	-115.0	-.000160
30.0	0.0300	-130.0	-.000250
40.0	-.0210	-135.0	-.000320
50.0	-.0215	-135.0	-.000380
60.0	-.0220	-140.0	-.000440
70.0	-.0230	-145.0	-.000530
80.0	-.0235	-147.0	-.000640
90.0	-.0240	-150.0	-.000760
100.0	-.0250	-155.0	-.000910
110.0	-.0270	-190.0	-.001060
120.0	-.0300	-205.0	-.001170
130.0	-.0340	-220.0	-.001230
140.0	-.0390	-250.0	-.001280
150.0	-.0370	-210.0	-.001390
160.0	-.0350	-260.0	-.001480
170.0	-.0360	-270.0	-.001430
180.0	-.0370	-285.0	-.001120
190.0	-.0320	-250.0	-.001760
200.0	-.0340	-330.0	-.001480
210.0	-.0290	-310.0	-.001210
220.0	-.0280	-270.0	-.000900
230.0	-.0210	-210.0	-.000610
240.0	-.0230	-160.0	-.000410
250.0	-.0170	-100.0	-.000190
260.0	-.0140	-70.0	-.000110
270.0	-.0140	-60.0	-.000070
280.0	-.0130	-45.0	-.000050
290.0	-.0100	-41.0	-.000030
300.0	-.0070	-35.0	-.000020

TRANSFER ORBIT ELEMENTS
INCLINATION = 21.500000000021 DEG
ECCENTRICITY = .5945937213[illegible]
TRUE ANOMALY AT ENTRY = -19.39+40407804 DEG

INERTIAL POSITION AND VELOCITY AT ENTRY
R(I) = [illegible] METERS
R(J) = [illegible] METERS
R(K) = [illegible] METERS
V(I) = 11[illegible] METERS/SEC
V(J) = [illegible] METERS/SEC
V(K) = [illegible] METERS/SEC

VELOCITY ERROR = -10.
FLIGHT PATH ANGLE ERROR = .002
MEASURED ACCELERATION ERROR = .1

ACTUAL VEHICLE TRAJECTORY

TIME (SECONDS)	ALTITUDE (METERS)	VELOCITY (M/SEC)	GAMMA (DEGREES)	DENSITY (KG/M3)	BETA COMMAND (DEGREES)	INCLINATION (DEGREES)
4.00	11[illegible]51.3	10[illegible]1.31	-4.3[illegible]63	.1[illegible]191E-05	86.8	21.5003
8.00	113406.3	10[illegible]7.95	-4.2101	.13[illegible]7E-05	98.3	21.5009
12.00	11[illegible]4.5	10[illegible]6.40	-4.0533	.2[illegible]E-05	91.1	21.5017
15.00	113225.4	10[illegible]6.62	-3.9163	.42[illegible]E-05	88.7	21.5028
20.00	113292.2	10210.55	-3.7591	.52[illegible]E-05	88.7	21.5046
24.00	113362.2	10[illegible]2.12	-3.6218	.9[illegible]1E-05	89.5	21.5071

28.00	101175.6	10203.21	-3.4746	.127563E-05	90.5	21.5107
32.00	97715.5	10203.79	-3.3270	.175331E-05	91.2	21.5157
36.00	94399.2	10203.41	-3.1798	.245725E-05	92.2	21.5227
40.00	91197.7	10202.14	-3.0328	.337553E-05	93.7	21.5322
44.00	88100.9	10199.63	-2.8854	.463619E-05	93.8	21.5450
48.00	85078.8	10195.95	-2.7405	.599371E-05	93.3	21.5519
52.00	82141.1	10190.57	-2.5951	.765511E-05	92.2	21.5841
56.00	79288.0	10181.25	-2.4498	.983956E-05	90.5	21.6123
60.00	76509.9	10170.16	-2.3043	.126271E-04	91.3	21.6492
64.00	73816.5	10155.82	-2.1592	.154356E-04	92.1	21.6948
68.00	71205.9	10137.73	-2.0141	.198241E-04	92.8	21.7510
72.00	68669.9	10115.39	-1.8694	.230647E-04	93.3	21.8192
76.00	66203.7	10088.37	-1.7245	.275312E-04	89.9	21.9010
80.00	63803.5	10056.24	-1.5814	.324421E-04	86.7	21.9977
84.00	61467.2	10019.71	-1.4366	.376830E-04	84.1	22.1101
88.00	59192.9	9975.62	-1.3071	.431548E-04	82.2	22.2384
92.00	56978.2	9926.97	-1.1535	.486395E-04	83.7	22.3823
96.00	54820.3	9872.97	-1.0050	.541235E-04	85.2	22.5437

100.00	*2530.5	8814.04	-.8526	.5023?9E-04	35.5	22.7204
104.00	*1087.*	9710.70	-.7276	.5407?4E-04	37.7	22.9112
108.00	*1577.6	9537.61	-.5998	.6834?9E-04	38.9	23.1145
112.00	*1174.0	9513.50	-.4403	.7283?4E-04	90.0	23.3281
115.00	*0390.2	9561.14	-.3594	.7503?7E-04	91.0	23.5493
120.00	*0774.2	9[illegible].29	-.2527	.77[illegible]5E-04	91.7	23.777+
124.00	*0535.0	9302.59	-.1720	.7913?3E-04	92.3	24.0086
128.00	*0451.5	9318.00	-.0843	.8025?5E-04	92.6	24.2415
132.00	*0423.5	9263.54	-.0026	.80?170E-04	92.6	24.-741
136.00	*0447.0	9170.74	.0750	.8053?4E-04	92.2	24.7048
140.00	*0514.0	9049.13	.1490	.7903?5E-04	90.1	24.9321
144.00	*0539.0	8979.55	.2291	.7875?4E-04	88.9	25.1547
148.00	*0603.2	8972.23	.3091	.7703?5E-04	88.4	25.3711
152.00	*1025.1	8907.53	.3951	.7405?1E-04	88.3	25.5802
156.00	*1236.7	8839.72	.4585	.7247?2E-04	92.9	25.7809
160.00	*1545.0	8776.97	.5115	.6961?3E-04	95.2	25.9724
164.00	*1910.5	8721.36	.5529	.6664?2E-04	95.7	26.1540
168.00	*2252.3	8668.86	.5913	.6359?0E-04	95.5	26.3260

172.00	[illegible]	[illegible]	.5281	.505122E-04	91.7	26.4387
176.00	[illegible]	[illegible]	.5730	.574139E-04	89.3	26.6428
180.00	[illegible]	[illegible]	.7216	.542363[illegible]-04	93.1	26.7878
184.00	[illegible]	[illegible]	.7704	.511414E-04	88.0	26.9237
188.00	[illegible]	[illegible]	.8105	.481054E-04	90.4	27.0505
192.00	[illegible]	[illegible]	.8746	.449143E-04	92.0	27.1689
196.00	[illegible]	[illegible]	.9374	.419193E-04	92.8	27.2788
200.00	[illegible]	[illegible]	.9168	.390134E-04	92.9	27.3805
204.00	[illegible]	[illegible]	.9446	.362598E-04	89.9	27.4747
208.00	[illegible]	[illegible]	.9758	.335109E-04	89.8	27.5613
212.00	[illegible]	[illegible]	1.0063	.310337[illegible]-04	89.3	27.6422
216.00	[illegible]	[illegible]	1.0357	.287024E-04	91.0	27.7151
220.00	[illegible]	[illegible]	1.0609	.264426E-04	97.1	27.7840
224.00	[illegible]	[illegible]	1.0825	.243197E-04	99.3	27.8461
228.00	[illegible]	[illegible]	1.0961	.223356E-04	107.0	27.9027
232.00	[illegible]	[illegible]	1.1065	.204394E-04	103.6	27.9531
236.00	[illegible]	[illegible]	1.1152	.187333E-04	100.0	27.9993
240.00	[illegible]	[illegible]	1.1251	.172235E-04	95.2	28.0423
244.00	[illegible]	[illegible]	1.1454	.157763E-04	88.0	28.0820

248.00	33185.4	8128.25	1.1561	.1442764E-04	80.7	28.1183
252.00	33253.6	8117.93	1.1305	.1317756E-04	92.9	28.1510
256.00	33272.5	8108.45	1.2069	.1219376E-04	104.5	28.1812
260.00	33213.1	8099.75	1.2119	.1083727E-04	117.3	28.2077
264.00	33087.1	8091.80	1.2215	.9954485E-05	128.0	28.2287
268.00	32907.9	8084.50	1.2257	.9153329E-05	135.9	28.2491
272.00	32742.1	8077.78	1.2356	.8233465E-05	90.4	28.2589
276.00	32603.0	8071.58	1.2510	.7413657E-05	77.3	28.2975
280.00	32503.1	8065.88	1.2702	.6793245E-05	66.2	28.3040
284.00	32424.1	8060.63	1.2916	.6162322E-05	71.8	28.3179
288.00	32356.1	8055.78	1.3128	.5537771E-05	77.6	28.3310
292.00	32287.8	8051.31	1.3279	.5041463E-05	81.7	28.3432
296.00	32218.4	8047.17	1.3436	.4551114E-05	83.7	28.3544
300.00	32147.2	8043.35	1.3585	.4103314E-05	82.3	28.3645
304.00	32073.5	8039.81	1.3716	.3696543E-05	84.5	28.3736
308.00	31996.5	8036.53	1.3835	.3325643E-05	104.0	28.3817
312.00	31925.6	8033.48	1.3947	.2991143E-05	100.3	28.3888
316.00	31850.5	8030.64	1.4052	.2691772E-05	101.1	28.3951
320.00	31771.4	8027.99	1.4168	.2422445E-05	93.9	28.4009

324.00	37098.7	8025.59	1.4290	.216381E-05	87.5	28.4052
328.00	37882.7	8023.17	1.4417	.193384E-05	82.6	28.4103
332.00	38713.6	8020.93	1.4547	.173598E-05	87.1	28.4151
335.00	39531.5	8018.91	1.4571	.155270E-05	91.0	28.4139
340.00	100356.0	8016.55	1.4702	.136750E-05	94.9	28.4223
344.00	101187.1	8015.08	1.4910	.123377E-05	95.4	28.4253
348.00	102024.4	8013.31	1.5025	.110592E-05	97.4	28.4250
352.00	102858.0	8011.61	1.5140	.984371E-05	96.4	28.4303
356.00	103717.8	8009.99	1.5256	.877133E-05	95.7	28.4325
360.00	104577.0	8008.41	1.5371	.780333E-05	95.1	28.4343
364.00	105436.4	8006.93	1.5485	.693701E-05	95.9	28.4359
368.00	106305.0	8005.43	1.5600	.616161E-05	95.0	28.4375
372.00	107173.8	8004.01	1.5713	.546823E-05	94.2	28.4388
375.00	108060.8	8002.52	1.5327	.484373E-05	79.3	28.4400
380.00	108943.1	8001.27	1.5943	.429325E-05	60.0	28.4410
384.00	109841.8	7999.96	1.6051	.380265E-05	50.0	28.4413
388.00	110741.0	7998.64	1.6176	.336312E-05	50.0	28.4425
392.00	111648.4	7997.35	1.6295	.297179E-05	50.0	28.4431
396.00	112561.1	7996.09	1.6410	.262377E-05	60.0	28.4435

400.00	113450.2	7944.34	1.6524	.231445E-05	71.8	28.4441
404.00	114405.4	7993.60	1.6577	.223383E-05	94.9	28.4445
408.00	114736.7	7932.37	1.6747	.179541E-05	105.5	28.4450
412.00	115274.0	7931.15	1.6855	.156170E-05	109.9	28.4454
415.00	117217.1	7929.94	1.6963	.175775E-05	115.1	28.4457
420.00	118165.1	7928.73	1.7071	.122331E-05	120.0	28.4459

```
DENSITY VARIATION = 1.
ACTUAL APOGEE ALTITUDE = 727.236955792 KM

1  CSP     12/7?? L4146       CYBR CMR? 01/01/77
 19.28.27.?JOB??.  FROM    /??
 19.28.27.??  00101406 WORDS - FILE INPUT  , DC 01
 19.28.27.?JO,T???,STCS?. ?????15,CHAMBERS,4175
 19.28.28.ATTACH,AFIT,AFITSUBROUTINES,ID=AFIT.
 19.28.28.?? CYCLE NO. = 002
 19.28.29.LIBRARY,AFIT.
 19.28.29.???,????.
 19.28.?9.????
 19.28.42.     2.304 CP SECONDS COMPILATION TIME
 19.28.42.L??.
 19.28.57.     ??? TH??1
 19.28.57.     7.093 CP SECONDS EXECUTION TIME
 19.28.57.??  00105352 WORDS - FILE OUTPUT , DC 40
 19.28.57.??   17920  WORDS  (   17920 MAX USED)
 19.28.57.???  ?3300  WORDS MAXIMUM
 19.28.57.???       7.091 ???.        3.073 ADJ.
 19.28.57.???       4.547 ???.        2.292 ADJ.
 19.28.57.???     203.21? KWS.        1.?63 ADJ.
 19.28.57.????                        7.032
 19.28.57.????                         .42
 19.28.57.??      13.534 ???.      DATE 02/03/77
 19.28.57.??  END OF JOB, ??  ??60416.
0
```

Vita

Robert J. Chambers, Jr., was born on May 30th, 1948 in Orange, New Jersey. He graduated from Mountain High School, West Orange, New Jersey in June, 1966 and entered the United States Air Force Academy, Colorado. He graduated in June, 1970, receiving a commission as a Second Lieutenant and a Bachelor of Science Degree, with majors in Astronautics and in Engineering Sciences.

After attending pilot training at Craig AFB, Alabama he was assigned to Rhein-Main Air Base, Federal Republic of Germany. While stationed here he flew as a squadron pilot in the C-130 aircraft, and later the C-131/T-29 aircraft. In 1975 he was selected to attend the Air Force Institute of Technology and entered in August of that year.

Permanent Address: 2105 Cherry Hill Drive
Arlington Heights, Illinois 60004

This thesis was typed by the author.

UNCLASSIFIED

SECURITY CLASSIFICATION OF THIS PAGE *(When Data Entered)*

REPORT DOCUMENTATION PAGE		READ INSTRUCTIONS BEFORE COMPLETING FORM
1. REPORT NUMBER GA/EE/77-1	2. GOVT ACCESSION NO.	3. RECIPIENT'S CATALOG NUMBER
4. TITLE *(and Subtitle)* Navigational Accuracy Requirements of Aeromaneuvering Space Vehicles		5. TYPE OF REPORT & PERIOD COVERED MS Thesis 6. PERFORMING ORG. REPORT NUMBER
7. AUTHOR(s) Robert J. Chambers, Jr. Capt USAF		8. CONTRACT OR GRANT NUMBER(s)
9. PERFORMING ORGANIZATION NAME AND ADDRESS Air Force Institute of Technology (AFIT-EN) Wright-Patterson AFB, Ohio 45433		10. PROGRAM ELEMENT, PROJECT, TASK AREA & WORK UNIT NUMBERS
11. CONTROLLING OFFICE NAME AND ADDRESS		12. REPORT DATE March, 1977 13. NUMBER OF PAGES 64
14. MONITORING AGENCY NAME & ADDRESS *(if different from Controlling Office)*		15. SECURITY CLASS. *(of this report)* UNCLASSIFIED 15a. DECLASSIFICATION/DOWNGRADING SCHEDULE

16. DISTRIBUTION STATEMENT *(of this Report)*

Approved for Public Release; Distribution Unlimited

17. DISTRIBUTION STATEMENT *(of the abstract entered in Block 20, if different from Report)*

18. SUPPLEMENTARY NOTES

Approved for Public Release, IAW AFR 190-17

JERRAL F. GUESS, Capt, USAF, Director of Information

19. KEY WORDS *(Continue on reverse side if necessary and identify by block number)*

Lifting Bodies
Lifting Reentry Vehicles
Lifting Reentry
Maneuverable Reentry Vehicles

20. ABSTRACT *(Continue on reverse side if necessary and identify by block number)*

A preliminary investigation was conducted to determine the navigational accuracy required by the Aeromaneuvering Orbit-to-Orbit Shuttle (AMOOS) during the atmospheric phase of flight. The guidance scheme, which is the same as the one developed by Lockheed in the original AMOOS study, uses the parameters of velocity, flight path angle, and density altitude to correct to a nominal trajectory. Density altitude is obtained from atmospheric density, which is calculated from vehicle acceleration. Errors in velocity,

DD FORM 1 JAN 73 1473 EDITION OF 1 NOV 65 IS OBSOLETE

UNCLASSIFIED

SECURITY CLASSIFICATION OF THIS PAGE *(When Data Entered)*

flight path angle, and acceleration were introduced into a three-degree of freedom computer simulation of the vehicle trajectory using bank angle commands generated by the guidance equations. Deviations from standard atmospheric density were taken into account.

The maximum errors allowable that still permitted the vehicle to attain its phasing orbit apogee altitude of 720 km (±100 km) were determined. Three types of error were investigated: constant, sinusoidal, and random. For time-varying errors the frequency dependence was examined, as was cross-coupling of errors.

It was concluded that the guidance scheme can tolerate fairly large errors and still guide to an acceptable apogee altitude. The navigational accuracy required for the atmospheric phase of flight is within the capability of present day astrionics.